

KADIR HAS UNIVERSITY
GRADUATE SCHOOL OF SCIENCE AND ENGINEERING



DE NOVO SELECTIVE INHIBITOR DESIGN TO NEURONAL NOS
ENZYME AND EXPLORATION OF THE BINDING SITE

ALİ BORA BÜYÜKTÜRK

May, 2013

DE NOVO SELECTIVE INHIBITOR DESIGN TO
NEURONAL NOS ENZYME
AND EXPLORATION OF THE BINDING SITE

ALİ BORA BÜYÜKTÜRK

B.S. and MS. Teaching Physics, Boğaziçi University, 2004

B.S., Computer Science, Istanbul Bilgi University, 2010

M.S., Computational Biology and Bioinformatics,
Kadir Has University, 2013

Submitted to the Graduate School of Science and Engineering
in partial fulfillment of the requirements for the degree of
Master of Science
in
Computational Biology and Bioinformatics

KADIR HAS UNIVERSITY

May, 2013

KADIR HAS UNIVERSITY GRADUATE SCHOOL OF SCIENCE AND
ENGINEERING

DE NOVO SELECTIVE INHIBITOR DESIGN TO NEURONAL NOS
ENZYME AND EXPLORATION OF THE BINDING SITE

ALİ BORA BÜYÜKTÜRK

APPROVED BY:

Prof. Dr. KEMAL YELEKCI
Thesis Supervisor
Kadir Has University

Asst. Prof. Dr. EBRU DEMET AKTEN AKDOĞAN
Kadir Has University

Prof. Dr. KUTLU ÜLGEN
Boğaziçi University

APPROVAL DATE: 15/05/2013

“I, Ali Bora Büyüktürk, confirm that the work presented in this thesis is my own. Where information has been derived from other sources, I confirm that this has been indicated in the thesis.”

Ali Bora Büyüktürk

DE NOVO SELECTIVE INHIBITOR DESIGN TO NEURONAL NOS ENZYME AND EXPLORATION OF THE BINDING SITE

ABSTRACT

Neural Nitric Oxide Synthase (nNOS) is an enzyme that plays a significant role in neural signal transmission among brain cells by carrying on Nitric Oxide(NO) generation.

nNOS is one of the member of Nitric Oxide Synthase (NOS) enzyme family and has three isoforms; nNOS, eNOS and iNOS. Since NO is a highly reactive compound, NOS isozymes have many distinct functionalities on neural, endothelial and immune systems respectively. Despite these functionalities, their binding sites show great similarities and hence it became a challenge to design a selective inhibitor to them.

Revealing of crystallographic structures of NOS isoenzymes set a foundation for in silico inhibitor design and computational modeling studies. We applied lead and fragment based de novo design techniques and carried on a series of computational docking operations on the NOS isoforms to discover an nNOS selective leading inhibitor against iNOS and eNOS. Utilizing virtual screening (VS) methods on different software environments we selected suitable lead scaffolds, added fragments, developed candidate ligands and applied leading docking algorithms on these ligands. We compared our ligands with experimental leading compounds defined on the related literature. Finally, we explored the binding sites and stated the properties of cavities and specific amino acids.

Keywords: nNOS, eNOS, iNOS, Nitric Oxide Syntheses, docking, scoring, molecular modeling, in silico screening, protein alignment, active site analysis

NÖRONAL NOS ENZİMİNE DE NOVO SEÇİLİMLİ İNHİBİTÖR TASARIMI VE BAĞLANMA BÖLGELERİNİN ARAŞTIRILMASI

ÖZET

Nöral Nitrik Oksit Sentaz(nNOS) Nitrik Oksit (NO) üretimini devam ettirerek beyin hücreleri arasında nöral sinyal iletiminde önemli rol oynayan bir enzimdir. nNOS Nitrik Oksit Sentaz (NOS) enzim ailesinin bir üyesidir ve üç izoformu bulunmaktadır; nNOS, eNOS ve iNOS. NO hayli reaktif bir bileşik olduğundan NOS izozimlerinin sırasıyla nöral, endotelyal ve bağışıklık sistemlerinde birçok ayırıcı fonksiyonellikleri vardır. Bu fonksiyonelliklerine rağmen bağlanma bölgeleri büyük benzerlikler gösterirler ve bu yüzden onlar seçici inhibitörler tasarlamak zorlayıcıdır.

NOS izozimlerinin kristalografik yapılarının açığa çıkması in silico inhibitör tasarımı ve hesapsal modelleme çalışmaları için bir temel oluşturmuştur. iNOS ve eNOS'a karşı nNOS seçimli bir öncü inhibitör keşfetmek için NOS izoformları üzerinde, öncü ve parça temelli de novo tasarım tekniklerini uyguladık ve bir seri hesapsal doklama operasyonu yürüttük. Farklı yazılım ortamlarında Sanal Tarama (VS) methodlarını kullanarak, uygun öncü iskelet yapılarını seçip, parçalar ekleyip, aday ligandlar geliştirdik ve önde gelen doklama algoritmalarını uyguladık. Literatürde tanımlı öncü deneysel bileşiklerin sonuçlarıyla ligandlarımızı kıyasladık. Son olarak, bağlanma bölgelerini araştırıp kavite ve belirli amino asitlerin özelliklerini ortaya koyduk.

Anahtar Kelimeler: nNOS, eNOS, iNO, Nitrik Oksit Sentaz, doking, skorlama, moleküler modelleme, in silico tasarım, protein hizalama, aktif bölge analizi

ACKNOWLEDGEMENTS

Thank you dear Prof. Dr. Kemal Yelekçi. I am glad that I had such an advisor that gave me many handy advices in the most patient and understanding way. Thank you dear Nurdan Kayrak. You never fail to introduce your neat and clear organization abilities during the crucial research steps. Thank you my dear family. You were always positive and supportive for this chronic lifelong student. Lastly, thank you Serkan Altuntaş for your last minute on time help.

Table of Contents

1	Introduction	12
1.1	Drug Discovery	12
1.2	Nitric Oxide (Nitrogen Monoxide, NO)	13
1.3	Nitric Oxide Synthase (NOS) Enzyme	15
1.3.1	NOS Structures	15
1.3.2	NOS Cofactors.....	17
1.3.3	NOS Functionality.....	19
1.4	NOS Literature	20
2	Methodology	24
2.1	Tools.....	26
2.1.1	Spartan	26
2.1.2	AccelrysDS	26
2.2	Docking Methodologies.....	27
2.2.1	Protein and ligand Preparation.....	27
2.2.2	AutoDock Methodology	27
2.2.3	CDock Methodology	28
2.3	De Novo Design.....	30
2.3.1	Library Generation.....	30
2.3.2	De Novo Lead Discovery	31
2.3.3	Fragment-based Lead Discovery.....	32
2.3.4	Parameters and Scoring.....	33
2.4	ADMET	34
2.5	In silico VS In vitro Case	34
2.6	Structural Alignment	38
3	Results	39
3.1	In silico vs. In vitro Case.....	39
3.1.1	Docking Results for nNOS	40
3.1.2	Docking Results for eNOS	43
3.2	De Novo Results	45
3.2.1	Lead Discovery Results	45
3.2.2	De Novo Fragment Based Discovery Results	46
3.3	ADMET Results.....	49
3.4	2D & 3D Results of De Novo Evolved Ligands.....	50
4	Conclusion.....	75

List of Tables

Table 1 NOS Receptors (resolutions units are in Angstrom A ⁰)	25
Table 2: ZINC Library properties	31
Table 3: 16 prominent selected ligands from recent NOS articles	37
Table 4: AutoDock results of 16 prominent ligands on 5 different nNOS crystal structures	40
Table 5: Log values of AutoDock Results of Table 4	40
Table 6: C-Dock results of 16 prominent ligands on 5 different nNOS crystal structures	41
Table 7: LibDock results of 16 prominent ligands on 5 different nNOS crystal structure	42
Table 8: AutoDock results of 16 prominent ligands on five different eNOS crystal structures	43
Table 9: Log values of AutoDock Results of Table 8	43
Table 10: C-Dock results of 16 prominent ligands on 5 different eNOS crystal structures	44
Table 11: LibDock results of 16 prominent ligands on 5 different eNOS crystal structures	45
Table 12: De Novo Lead Discovery (best ZINC molecules that will be used as a Lead in the Fragment based De Novo Stage).....	46
Table 13 Fragment Based Discovery drug candidates and their, Ludi Scores and	48
Table 14: AutoDock results of evolved drug candidates in Fragment based De Novo Design.	66
Table 15: NOS isozymes alignment results	67

List of Figures

Figure 1: Nitric Oxide displayed in "CPK" and "Ball & Stick" modes	13
Figure 2 : eNOS dimer and NtoC (blue to red) structures (1FOI)	15
Figure 3: iNOS dimer and NtoC (blue to red) structures (1NOD)	16
Figure 4 : nNOS dimer and NtoC (blue to red) structures (3N2R)	16
Figure 5 : NOS isozyme Active Sites, ligands and cofactors.....	17
Figure 6: NOS Cofactor Tetrahydrobiopterin (H4B) *5,6,7,8-Tetrahydrobiopterin *2-Amino-6-(1,2-ihydroxypropyl)-5,6,7,8-tetrahydro-4(1H)-pteridinone.....	18
Figure 7 NOS Cofactor Heme C ₃₄ H ₃₂ FeN ₄ O ₄ Protoporphyrin IX Containing FE	18
Figure 8-Conversion of L-Arginine to L-citrulline and nitric oxide (NO) catalyzed by the enzyme nitric oxide synthase.	19
Figure 9: Stereo views of crystal structures of nNOS and eNOS binding to L-Arginine	22
Figure 10 Docking in AccelrysDS: Cavity and chosen binding site sphere is shown	29
Figure 11: nNOS AutoDock results chart of Table 5 denoting logarithmic behavior of inhibition constants	41
Figure 12 : eNOS AutoDock results chart of Table 9. denoting logarithmic behavior of inhibition constants	44
Figure 13: ADMET results of molecules evolved in fragment De Novo	49
Figure 14 : 2D&3D images of 1NSI and zinc00151524_evo3 interaction.....	50
Figure 15: 2D&3D images of 1NSI and zinc00151524_evo7 interaction.....	51
Figure 16: 2D&3D images of 1NSI and zinc00151524_evo10 interaction.....	52
Figure 17: 2D&3D images of 1RS7 and 1RS7_zinc04859564_evo5.....	53
Figure 18: 2D&3D images of 1RS7 and 1RS7_zinc04859564_evo6 interaction.....	54
Figure 19 : 2D&3D images of 1RS7 and 1RS7_zinc04859564_evo10 interaction.....	55
Figure 20: 2D&3D images of 1RS7 and 1RS7_zinc42689701_evo5 interaction.....	56
Figure 21: 2D&3D images of 1RS7 and 1RS7_zinc42689701_evo6 interaction.....	57
Figure 22: 2D&3D images of 1RS7 and 1RS7_zinc42689701_evo10 interaction.....	58
Figure 23-2D interaction image 3DQS and 3DQS_zinc00081090_Evo8	59
Figure 24 nNOS active site cavity and positioning of the close residues	68
Figure 25 Five structurally aligned eNOS enzymes	69
Figure 26eNOS enzymes with its cofactors and cavity	69
Figure 27 Two structurally aligned iNOS enzymes	70
Figure 28 iNOS enzymes with its cofactors and cavity	70
Figure 29Ten structurally aligned nNOS enzymes	71
Figure 30 nNOS enzymes with its cofactors and cavity	71
Figure 31: nNOS Cavity	72
Figure 32: eNOS Cavity.....	73
Figure 33: iNOS Cavity	74

List of Abbreviations

Nitric Oxide.....	NO
Nitric Oxide Synthases	NOS
Neuronal Nitric Oxide Synthases	nNOS
Endothelial Nitric Oxide Synthases	eNOS
Inducible Nitric Oxide Synthases	iNOS
Tetrahydrobiopterin	BH4
L-arginine	L-Arg
Accelrys Discovery Studio	AccelrysDS
Root Mean Square Deviation/Distance	RMSD
Nicotinamide adenine dinucleotide phosphate	NADP
Flavin adenine dinucleotide	FAD
Flavin mononucleotide	FMN
Tetrahydrobiopterin	BH4
Human Intestinal Absorption	HIA
Interferon-gamma	IFN- γ
Tumor necrosis factor	TNF
Transforming growth factor beta	TGF- β
Interleukin-4	IL-4
Food and Drug Administration.....	FDA
New Drug Application	NDA
High Throughput Screening	HTS

1 Introduction

1.1 Drug Discovery

Drug discovery and travel of a drug to a pharmacy shelves are long processes taking average twelve to fourteen years. Thousands of molecules have to be screened and tested on computers, in laboratories and on the living bodies. The successful drug candidates should be tested on firstly on tissues, animals and then finally on humans. Several thousands of patients are observed in clinics to learn more about toxicity, absorption, insolubility, metabolic reactions to overcome the side effects, deciding safety and tolerability and clarifying the dosage regimens. Elimination of unwanted activities and amplification of desired activities of a drug are the main concerns before NDA and FDA approvals. Luckily, recent computer advancements accelerated the initial step of these long procedures that more probable drug candidates are chosen in a more efficient way for the further steps.

Human body is a huge system of molecules. A compound may have many interaction with many other molecules in the body. It is not easy to let a compound function only in one way without harming or interacting other molecules and systems in the body. Hence, one of the most challenging aspects of drug design is to find a drug which is selectively acts on the intended specific mechanism of a system without throwing any side effect. For instance, the NO molecule is used in neurotransmission, endothelial vasodilation and immune defense system mechanisms in the body. Very active molecule with many regulatory effects nitric oxide is selected as the molecule of the year in 1992 (Figure 1). So it is very difficult to develop a drug which is selectively effective only on one of

these NO containing system mechanisms. For instance, the drug “Sildenafil” citrate, popularly known as Viagra is discovered while working on heart diseases. It is discovered as a side effect because it was stimulating penile erections through the nitric oxide pathway.

In this study, we would like to contribute to the search of a noval selective drug inhibitor molecule acting on NO. Contrary to Viagra, we wish to find a drug candidate, which is effective on neural NOS which process on brain neurotransmitters rather than those process on immune or endothelial systems.

1.2 Nitric Oxide (Nitrogen Monoxide, NO)

Nitric oxide is an important intermediate free radical molecule that functions as a signaling and regulatory molecule in various pathological and physiological processes. NO is a subject of neuroscience, physiology, and immunology. NO is produced by NOS enzyme family in the body from L-Arginine amino acid. NO is also made by reduction of inorganic nitrate in bacteria.

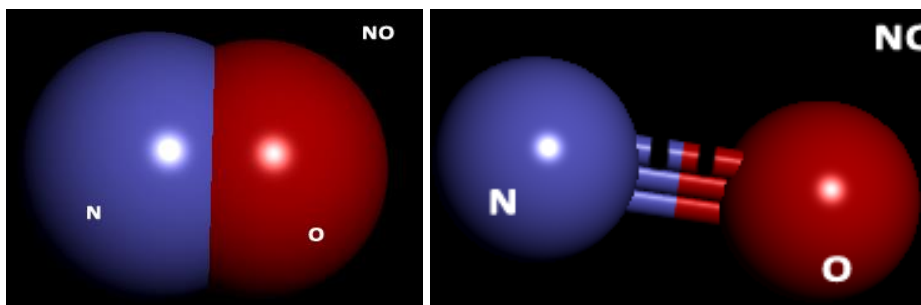


Figure 1: Nitric Oxide displayed in "CPK" and "Ball & Stick" modes

Nitric oxide has many benefits for human. Inner facing of blood vessels (Endothelium) uses NO to relax nearby smooth muscles by signaling, hence increasing blood flow

causing vasodilation. It decreases blood pressure in endothelial cells (Fleming & Busse, 2003). The production of nitric oxide is elevated in populations living at high altitudes, which helps these people avoid hypoxia by aiding in pulmonary vasculature vasodilation. Effects include vasodilatation, neurotransmission, modulation of the hair cycle, production of reactive nitrogen intermediates and penile erections. Nitric oxide can contribute to reperfusion injury when an excessive amount produced during reperfusion goes to a reaction with superoxide producing peroxy nitrite, which is a damaging oxidant (KA, 2012) . Contrary, inhaled nitric oxide has recovery effects against paraquat poisoning. This poisoning obstructs NOS metabolism by producing superoxide and damages lung tissues (Drummond, Cai, Davis, & Ramasamy, 2000). Low levels of nitric oxide production are important in protecting organs such as the liver from ischemic damage. Nitric oxide is considered an antianginal drug. it causes vasodilation, which can help with ischemic pain, known as angina, by decreasing the cardiac workload. By expanding the veins, nitric oxide drugs lower arterial pressure and left ventricular filling pressure. (Chirkov, 2001)

One of the generations of Nitric oxide (NO) is by monocytes, macrophages, and neutrophils as part of the human immune response destroys microorganisms and pathogens. NO is a free radicals and a toxic compound. When secreted against bacteria as an immune response, causes DNA damage and degradation of iron sulfur centers. NO might serve as an inflammation measurement device in asthma case. The level of exhaled NO reduction can be compared to air pollution exposure. (Batra, Chatterjee, & Ghosh, 2007)

NO regulates the release of neurotransmitters and is involved in synaptic plasticity, memory function and neuroendocrine secretion in neuronal cells. In our brain, under certain pathological conditions after certain ages produced excessive NO, causes tissue damage and oxidative stress. These complications are basis of diseases such as including rheumatoid arthritis, Alzheimer's disease, and Parkinson's disease. (Silverman R. B., 2009)

1.3 Nitric Oxide Synthase (NOS) Enzyme

Nitric Oxide Synthases (NOS) enzyme family members are enzymes, which catalyze the L-Arginine amino acid to nitric oxide (NO) and L-citrulline molecules. nNOS, eNOS and iNOS are the most common isozymes in the family (Figure 8).

1.3.1 NOS Structures

On average, NOS enzymes are 420 to 430 amino acid long proteins found mostly in dimer complexes. The structures are given in Figure 2, Figure 3 and Figure 4 as follows:

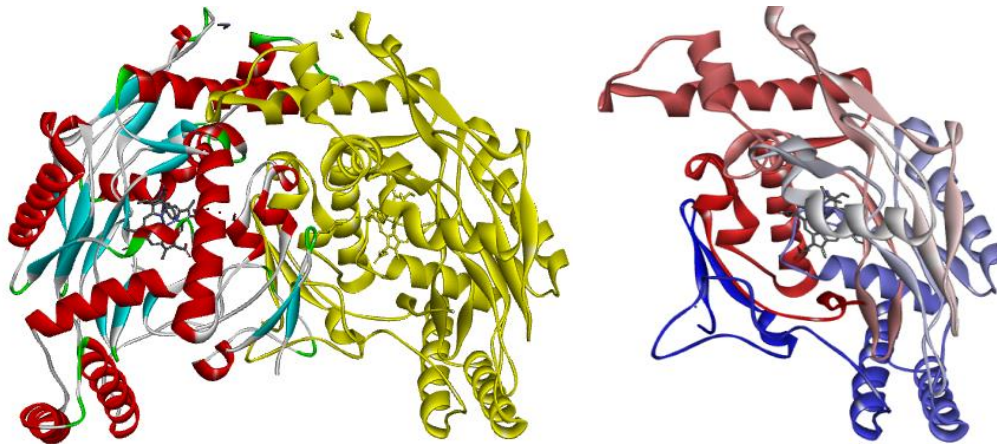


Figure 2: *eNOS* dimer and *NtoC* (blue to red) structures (1FOI)

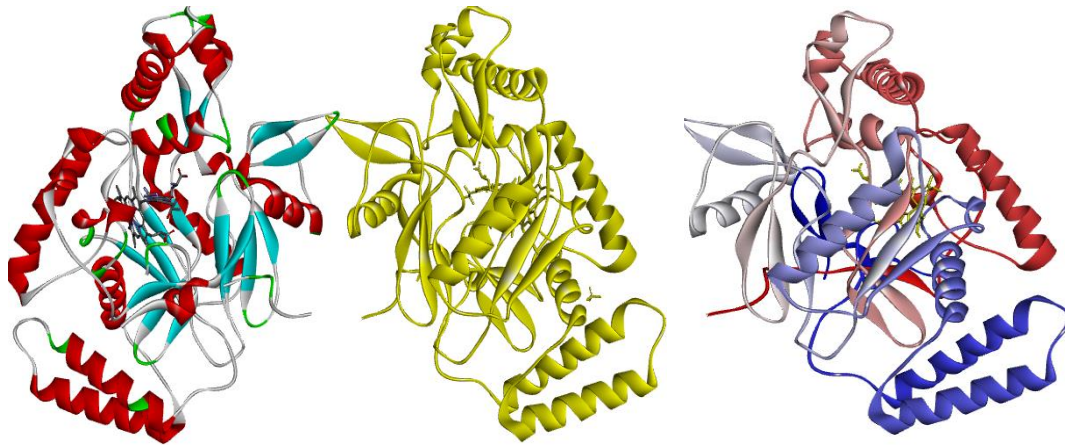


Figure 3: *iNOS* dimer and *NtoC* (blue to red) structures (1NOD)

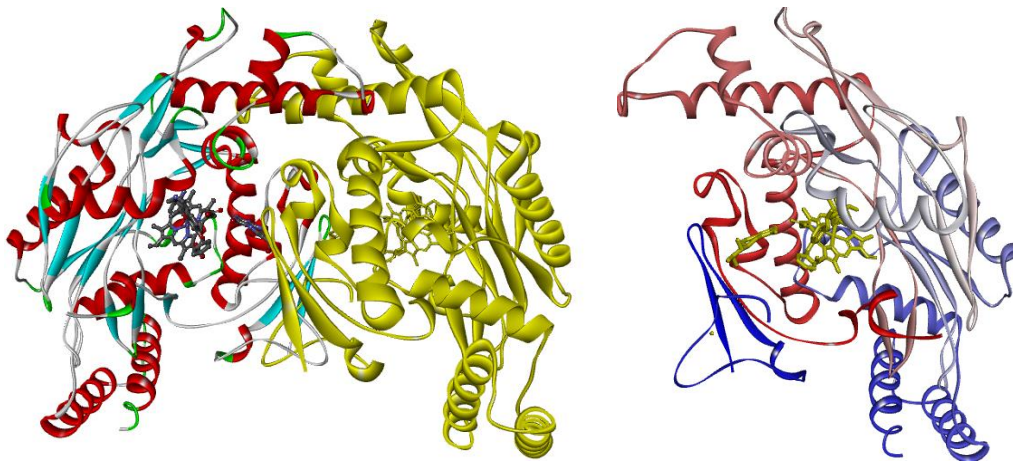
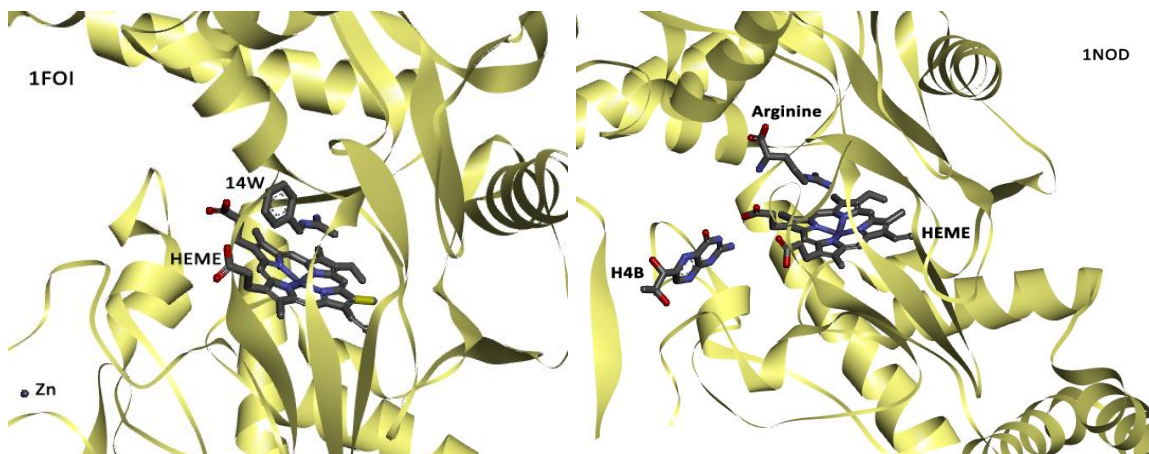


Figure 4: *nNOS* dimer and *NtoC* (blue to red) structures (3N2R)



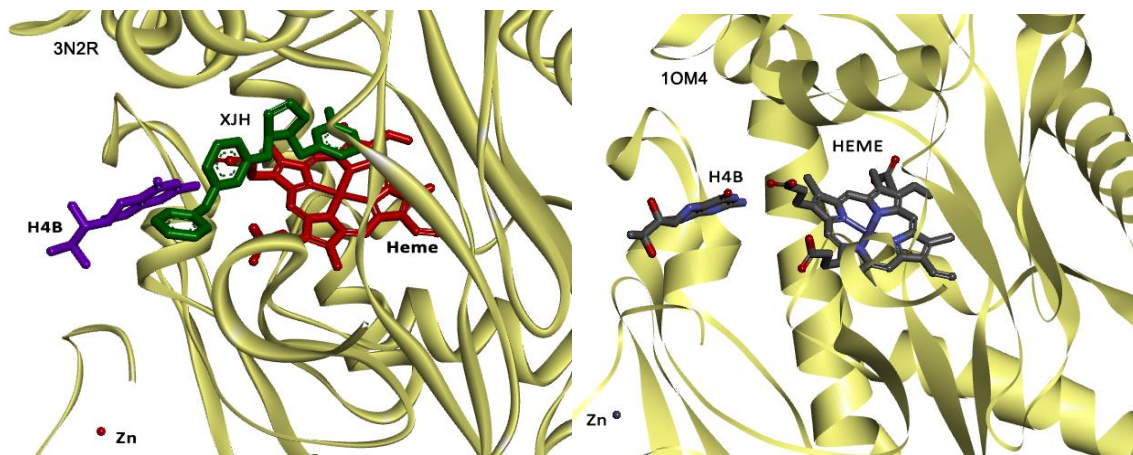


Figure 5 : NOS isozyme Active Sites, ligands and cofactors

1.3.2 NOS Cofactors

A cofactor is a molecule that is required for the biological activity of a protein. Loosely binding cofactors named coenzymes and tightly binding cofactors termed prosthetic groups. Apoenzyme is an inactive enzyme without the cofactor, whereas the holoenzyme is the complete enzyme with cofactors. NOS cofactors contribute conversion of guanidino nitrogen of L-Arg to NO. They are a Zn atom, a Heme and a Tetrahydrobiopterin (BH₄), Nicotinamide adenine dinucleotide phosphate (NADP), Flavin adenine dinucleotide (FAD) and Flavin mononucleotide (FMN) molecules.

Heme (Figure 7) is a an iron ion containing prosthetic group contained in the center of a large heterocyclic organic porphyrin ring, composed of four pyrrolic groups and methine bridges. Hemes are recognized as part of hemoglobin in blood, hemo-proteins such as myoglobin, cytochrome and catalase, etc.

Tetrahydrobiopterin (Figure 6) is a naturally occurring essential cofactor of the three aromatic amino acid hydroxylase enzymes, used in the degradation of amino acid

phenylalanine and in the biosynthesis of the neurotransmitters serotonin, melatonin, dopamine, noradrenaline, adrenaline. The role of BH4 in this enzymatic process is very critical that being a core cause of the neurovascular dysfunction that is the hallmark of circulation-related diseases such as diabetes.

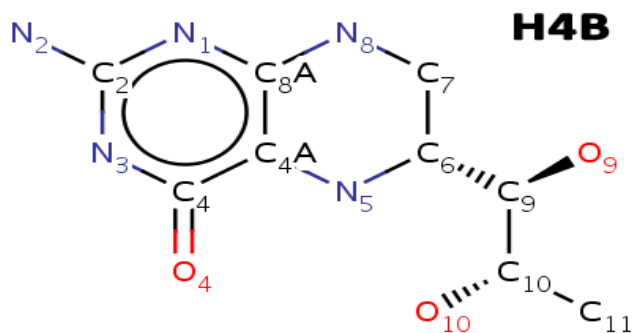


Figure 6: NOS Cofactor Tetrahydrobiopterin (H4B) *5,6,7,8-Tetrahydrobiopterin *2-Amino-6-(1,2-dihydroxypropyl)-5,6,7,8-tetrahydro-4(1H)-pteridinone

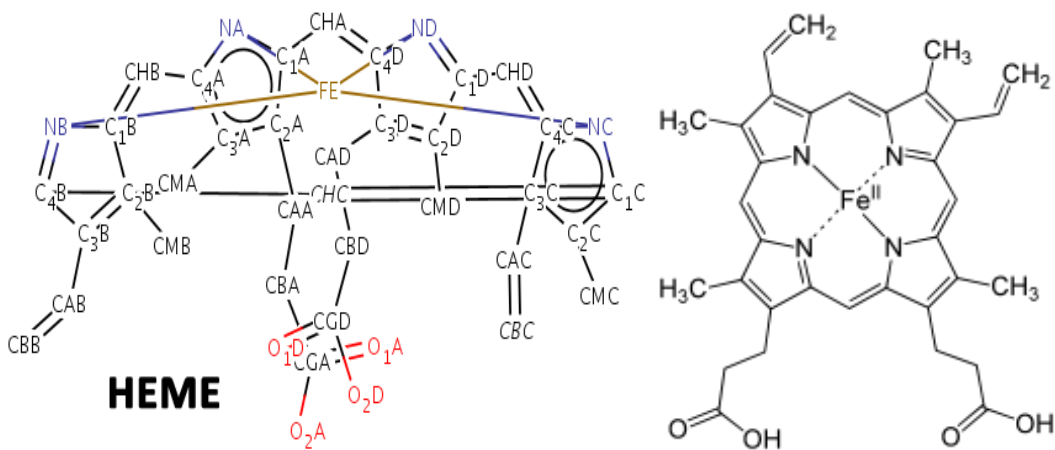
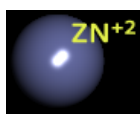


Figure 7 NOS Cofactor Heme $C_{34}H_{32}FeN_4O_4$ Protoporphyrin IX Containing FE



Crystal structures of these double-headed amino pyridine inhibitors in complexes with nNOS show unexpected and significant protein and Heme conformational changes induced by inhibitor binding that result in removal of the Tetrahydrobiopterin (H4B) cofactor and creation of a new Zn^{2+} pterin binding site. In

the dimer interface, Zinc tetrathiolate center helps dimer stabilization (Igarashi, et al., 2009). These changes are due to binding of a second inhibitor molecule that results in the displacement of H4B and the placement of the inhibitor pyridine group in position to serve as a Zn^{2+} ligand together with Asp, His, and a chloride ion. Binding of the second inhibitor molecule and generation of the Zn^{2+} site do not occur common in some of the eNOS and iNOS. (Silverman, Poulos, Jamal, Li, Xue, & Delker, 2010)

1.3.3 NOS Functionality

Nitric oxide producing NOS enzyme has three isoenzymic forms which of two is structural and the last one is inducible. While eNOS in endothelial cells produces NO to regulate blood pressure, nNOS in neuronal cells produces NO for neurotransmission and iNOS in macrophage cells being stimulated by pathogens produces NO to fight against infections and microorganisms. Under the presence of cofactors NADPH, FAD, FMN and BH4 (Figure 6) NOS enzyme produces NO by oxidation of L-Arginine terminal guanidino group. (Silverman & Zhu, 2008)

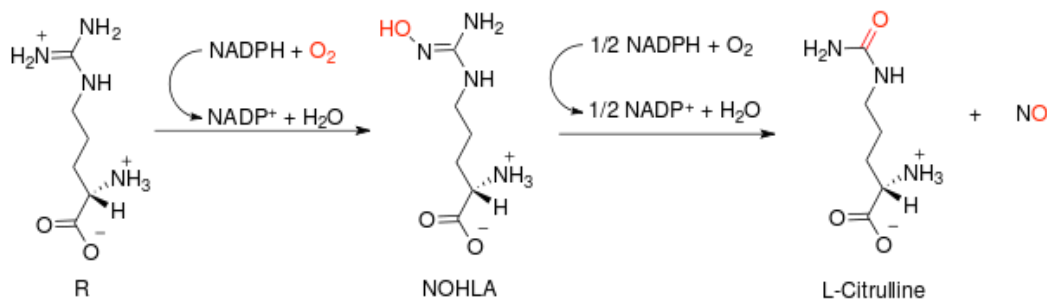
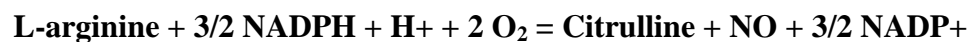


Figure 8 Conversion of L-Arginine to L-citrulline and nitric oxide (NO) catalyzed by the enzyme nitric oxide synthase.



Five cofactors are essential for catalyzes carried on by NOS isoenzymes. NADPH is in

reductase domain and transfers two electrons to FAD. FMN transfers one electron to Heme in oxygenase domain. BH₄ in oxygenase domain facilitates catalysis from L-Arginine to L-Citrulline. Zn, Glycerol (GOL) and two-water molecules' interactions are the other facilitators. (Silverman & Zhu, 2008)

Phagocytes are armed with iNOS. It is activated by IFN- γ or TNF as first and second signals respectively. Alternatively, TGF- β provides a strong, whereas IL-4 and IL-10 provide weak inhibitory signals. This way, the immune system regulates the armament of phagocytes playing role in inflammation and immune responses. (Teng, Zhang, Snead, & Catravas, 2002)

1.4 NOS Literature

From the beginning of 90's, many research-based pharmaceutical companies commence programs targeting nNOS selective compounds detection, because of the potential benefit of neurodegenerative diseases treatment (Erdal, Litzhger, Seo, Zuhu, Ji, & Silverman, 2005) . Before crystal structure of NOS enzyme discovered, basic approach was using L-Arginine substrate as lead compound and applying structural changes on it with the hope of selective binding analogues to nNOS, eNOS and iNOS (Igarashi, et al., 2009). Researches denote that the lack of selectivity is because of high similarity of substrates, active sites and reactions of these 3 enzymes. Any modifications on L-Arginine binding the active sites will have similar effects. A few compounds designed to bind as an anchor to active site looking for a difference from distant iron cofactor site tries to reach out second cavity of amino acids (Igarashi, et al., 2009).

A number of studies related to clarifying functional groups of lead compound

responsible with selectivity carried on. Biggest surprise in these studies was to show dipeptide analogue has weak potential and low selectivity. A sharp decrease noted by the need to amino group adding peptoid composed by adding carboxamide group. In addition, carboxamide excision lowers the selectivity. Consequently, the changes on carboxamide or nitroguanidine groups of lead compound will bring on selectivity increase (Silverman, Martasek, Roman, Huang, & Hui, 2000).

First crystal structures of iNOS and eNOS discovered at the end of 1990's by X-Ray Crystallography technique. Both isozymes' active sites are extremely similar. nNOS structure which will enlighten inhibitor selectivity was not definite until 2002. The important difference between nNOS and eNOS enzymes, with respect to eNOS in nNOS ligand places vertically whereas in eNOS there is an inclination (Figure 9). Lacking effects of absence of Nitric Oxide enzyme are observed on the transgenic mice for all NOS isoenzymes on (knock-out) as it is expected. (Silverman R. B., 2009) In the lights of these experiments, we can claim that without hypertensive effect of eNOS inhibition or without attenuating immune system strength iNOS inhibition, obtaining a selective nNOS inhibition will be protective effect upon neurodegenerative diseases.

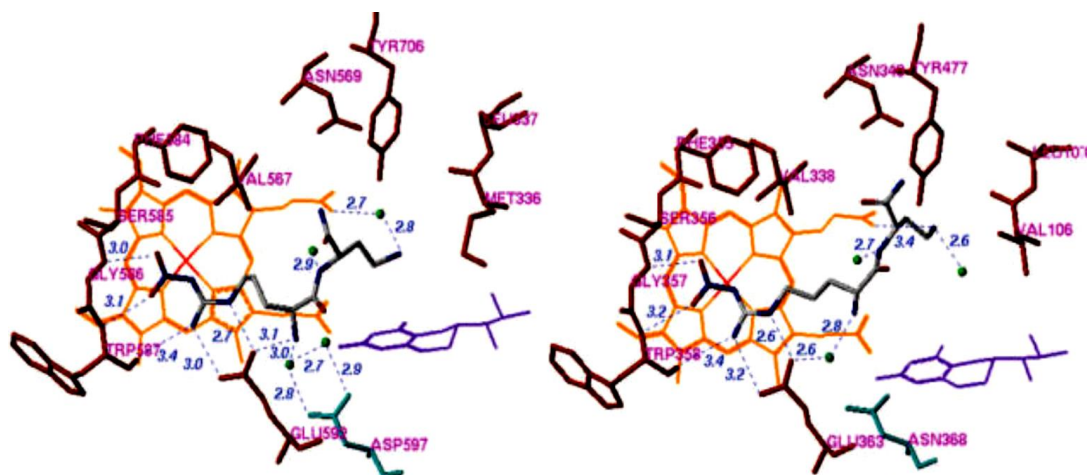


Figure 9: Stereo views of crystal structures of nNOS and eNOS binding to L-Arginine

The alpha-amino primer L-Nitroarginine group cannot be modified because electrical interaction between Asp597 and Glu592 amino acids of nNOS is active. All nNOS inhibitors nitroguanidino groups are bound to the same guanidino groups of nNOS arginine analogs (Poulos, Li, Raman, Martasek, & Masters, 2001). The main differences among nNOS to eNOS and iNOS and among active site amino acids can help designing selective inhibitors.

Characterization of active sites is done by observing molecular interaction fields derived from 10 different grid probe (GRID, 2002) and calculations of these fields by CPCA (consensus principal compound analysis) method. A conclusion is arrived as electrostatic and hydrophobic interactions are most dominant interactions (Westerhuis, Kourti, & Macgregor, 1998).

First computer modeling studies creates effects in the direction of "De novo" inhibitor design on the selective compounds classes on NOS isozyme caused more broader and new modeling approach. This approach called fragment hopping (H. et al. 2008). The

base of fragment hopping is to produce a minimal pharmacophoric element for each pharmacophore that isozyme selective and ligand binding sites take role. Five libraries are prepared named as base fragment, bioisostere, metabolic stability rules, toxicophore and side chain. These general libraries are used to match each pharmacophore to each minimal pharmacophoric element.

2 Methodology

In this study, we started with a literature scanning for NOS related articles published for the last 2 decades. We selected the best 16 ligands declared on the papers according to experimental laboratory results. We drew them from the scratch on AccelrysDS and minimized them into the energetically best conformations by AccelrysDS' clean geometry tool. In addition, for some failure docking result we repeated the same operation using Spartan programs and its minimization tool, which also introduces quantum calculations for a better output ligand file. In silico docking operations are carried out on these ligands to mimic the real world. We set CDOCKER and LibDock docking volumes fixed to 14 to 16nm radius spheres, and 56NM edged square in AutoDock by setting the center to Fe atom on the Heme. The lab results are compared to identify systems accuracy, calibration and validation for future library screenings. We downloaded 24 different NOS isozyme pdb files from RCSB protein databank. PDB files keeps the 3D coordinates of all the atoms of the molecule. 3PNE, 3PNF, 3PNG, 3PNH, 3SVP, 3SVQ were from latest articles that we only introduced them to the alignment operations since we were in the middle of study by the time. We used enzyme pdb files as their resolutions are given on the Table 1. We decided to use the enzyme pdb files referred in the articles that we have chosen our 16 promising ligands. Aiming to go for an HTS for de novo we wanted to keep only one enzyme from each isoform enzyme sets. So we docked all promising ligands to all enzymes and distributed to isoform graphs and pick the each one closest to experimental value which is more suitable to our in silico environment. We download ZINC fragment database that holds a million over molecular fragments and drug-like molecules. We moved further with a

series of de novo lead scaffold searches on AccelrysDS. Highest scored scaffolds are set aside and accepted as base scaffolds for the next fragment based de novo design.

Succeeding fragments based de novo design resulted with evolved new drug candidates for the cavities. This time, we went for a series of docking operations.

For this purpose, we used two different popular software tools to find the most probable potential inhibitor conformer based on binding affinity. We detected the most selective ligands for nNOS enzyme afterwards. At this point, we concerned metabolic functionality of new ligands so that we applied an ADMET test. Brain Blood Barrier passage capabilities are also important, since nNOS is a neural enzyme. Our test resulted with a table displaying five different measurement validation territory including BBB. Successful ligands falling into approved ADMET domains are observed under 2D and 3D visualization analysis for the conformer placement in the active site. Interactions are identified among ligands, cofactors and amino acids are stated. At the end, to observe the cavities in the binding sites of similar NOS isozymes, we applied a few structural alignments.

nNOS	Resolutions A⁰	nNOS	Resolutions A⁰	eNOS	Resolutions A⁰
1OM4	1.75	3B3M	1.95	3DQT	2.54
1P6I	1.9	3B3N	1.98	3DQS	2.03
1P6J	2	3PNE	1.97	1FOI	1.93
1QWC	2.3	3PNF	1.94	2NSE	2.34
1RS7	1.95	3PNG	1.88	3PNH	1.93
3B30	2.05	3SVF	1.98		
3DQR	2.4	3SVQ	2.18	iNOS	Resolutions A⁰
3N2R	1.9	3SVP	1.98	1NOD	2.6
3SVP	2.05			1NSI	2.55

Table INOS Receptors (resolutions units are in Angstrom A⁰)

2.1 Tools

- A RHEL5 server having Intel Quadro processor and nVidia G84 Quadro FX 1700 Graphics card
- An IBM workstation having Quadro core i7 processors.
- Three cores of 96core server is allocated for AutoDock processes. The visual screening jobs are submitted with qsub scripts
- Discovery Studio 3.1, Spartan 10.1, AccelrysDS CDocker and LibDock protocols, Autodock4.2. Raccoon interface and Spartan molecular modeling software.

2.1.1 Spartan

Spartan is a molecular modeling software program of Wavefunction Inc., which is capable of introducing quantum mechanics to the molecular computations. We utilized Spartan's minimization function by setting energy profile equilibrium geometries to semi-empiric geometry with PM3 model, which is suitable to identify conformational minima, and for determining the geometries of these minima. Spartan is introduced when a ligand conformation caused a system crash during docking.

2.1.2 AccelrysDS

Accelrys Discovery Studio is a client-server molecular simulation visual programming software suite built on a Pipeline Pilot developed by Accelrys Software Inc. It is very useful in developing novel therapeutic medicines. By licensing, Discovery Studio Accelrys Suite may contain docking protocols such as CDocker and LibDock that are widely used by computational chemists and biologists. (Sousa & Fernandes, 2006)

2.2 Docking Methodologies

2.2.1 Protein and ligand Preparation

Initially NOS crystal structures mentioned in the literature retrieved from protein databank. One of the monomer chains of the protein dimers are selected and the other is removed. Both water molecules and irrelevant substances like ammonium placed in the crystal complex obtained from protein databank are removed from the pdb files. We removed ligands as well without touching cofactors. The charge of central Heme Fe atom is set as +3 instead of +2 after breaking the bond in between cysteine amino acid located behind the Heme cofactor and Fe atom. Then, the hydrogen atoms are inserted. AccelrysDS tools correct distortions of the protein. Under the influence of a clean geometry short minimization, the bond angles and distances are optimized. Hence, these optimized pro-structures became suitable to insert candidate ligands to the active sides in the docking procedures. Pdb files are saved in “sd” format for CDocker and LibDock protocols. For the enzymes causing run time problems in other docking programs, we introduced Spartan’s ligand conformation optimization tools.

2.2.2 AutoDock Methodology

Genetic algorithms are search heuristics that mimics the process of natural evolution that routinely are used to generate useful solutions to optimization and search problems.

AutoDock uses a genetic algorithm for the conformational search. AutoDock docking environment uses a semi-empirical force field based on the AMBER force fields.

AutoDock uses a molecular mechanics model for enthalpic contributions. Van der Waals and hydrogen bonding, and an empirical model for entropic changes upon binding are

some examples. Each of these components are multiplied by empirical weights obtained from the calibration against a set of known experimental binding constants. For the conformational search, AutoDock uses a Lamarckian genetic algorithm. 70 independent runs are performed for each molecule. 300 distinct ligand conformers are initially generated and this population positioned randomly in the binding cavity. They are randomly assigned torsion angles to rotatable bonds and an overall rotation. Maximum 5 million energy evaluations are allowed for each docking. AutoGrid program pre-calculates 3D energy grid of equally spaced discrete points prior to docking for a rapid energy evaluation. We chose a grid box, with dimensions of 56*56*56 angstroms. It is centered at the iron atom contained in the center of a large heterocyclic organic ring of Heme group and covers the entire binding site and its neighboring residues. The distance between 2 grid points is set to 0.375 Å. Enzyme pdb files are converted to “pdbqt” files by Autodocktools.1.5.4 by program adding Gasteiger Charges aiming to use in AutoDock 4.2 program.

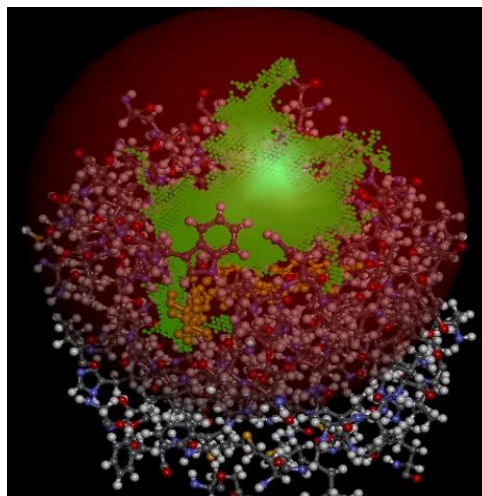
2.2.3 CDock Methodology

CDOCKER uses a molecular dynamics-based algorithm for the conformational search. Dynamic-based algorithms obtain their efficiency by solving and storing the answers to small problems that they usually trade off space for increased speed. Discovery Studio 3.0 CDOCKER protocol uses the CHARMM force fields and a molecular dynamics grid based docking algorithm, and elicits full ligand flexibility and reasonable computation times. It involves several random ligand conformations generation inside the target protein active site, following an MD-based simulated annealing composed of many heating and cooling procedures. Final refinement is an energy minimization. CDOCKER

makes use of soft-core potentials. They are effective in exploring the conformational spaces of small organics and macromolecules. The unbounded interactions that include electrostatics and van der Waals are softened at different levels, except during the final minimization step.

In CDOCKER, initially generates 10 random conformations replicas for each inhibitor in the active site of the target protein. Target is created as a spherical region with a diameter of 12Å and centered on the HEME molecule. Simulated annealing is performed using a flexible ligand and a rigid protein. The ligand-protein interactions are computed from grid extension 8.0. Random conformations are generated using 1000 molecular dynamic steps, while the system is heated up to 1000 K in 2000 steps. In the simulated annealing, the number of heating steps is set to 2000, the heating target temperature to 700K, whereas cooling steps to 5000, and the cooling target temperature to 300 K. The final refinement step of minimization is performed with full potential. Final minimized docking poses are then clustered, based on a heavy atom RMSD approach using a tolerance of 0.5Å. The final ranking is based on the total docking total energy, which is composed of the ligand's intramolecular energy and the ligand-protein interaction. The Discovery Studio-3.0 visualization tool is used to analyze the 10 top hit conformations (Brooks et al. 1983).

Figure 10: Docking in AccelrysDS: Cavity and chosen binding site sphere is shown



2.3 De Novo Design

In Latin, De Novo means "from the beginning". In our context, with De Novo design we will make predictions about new drug inhibitors using computational models without comparison to existing drugs. We will use compound libraries to generate scaffolds suitable to NOS cavities and then we will add additional groups to these leads from the fragment libraries. At the end, we will try to come up with new molecules, which will have correlated docking results to original NOS substrate.

2.3.1 Library Generation

In AccelrysDS, we generated standard Ludi libraries for De Novo Receptor and link libraries for De Novo Link and De Novo Evolution protocols by using ZINCv12 compound library. AccelrysDS generated Ludi str files for fragment topologies and trg files for specifying interaction types of functional groups. ZINC is a free database of commercially available compounds for virtual screening. They contain more than a million compounds. The Shoichet Laboratory in the Department of Pharmaceutical Chemistry at the University of California, San Francisco (UCSF), provides ZINC. We also contributed to ZINC library by 400 thousand fragments AccelrysDS libraries.

In ZINC database, there are three library subdomains of compound subsets. These are called "Standard", "Clean" and "inStock" subdomains. We have mainly used the inStock subdomain. Standard library subsets are popular subsets that appear commonly in the literature approximations. Clean subsets are what is left after problematic compounds in some assays are removed. InStock subsets are composed of the molecules, which are immediately available from stocks. These compound sets can be made in two

months' time. InStock library subsets are filtered into three groups. They are called “Lead-Like”, “Fragment-Like” and “Drug-Like” groups. Filtering criteria are as follows:

ZINC Libraries	Lead-like (Lead Now)	Fragment-like (Frag Now)
AccelrysDS De Novo	Lead Discovery	Fragment Based Lead Improvement
Compounds	1943551	400420
Date	2012-04-20	2012-04-16
octanol/water partition coefficients (xlogp)	< 3.5	<=3.5
Molecular weight (mwt)	>=250 & <= 350	<=250
Rotational bonds (rb)	<= 7	<= 5

Table 2: ZINC Library properties

2.3.2 De Novo Lead Discovery

We tried to find leader scaffolds to our NOS cavities to improve later by adding new small fragments onto them to find new drug candidates. The De Novo Receptor protocol is utilized to identify potential molecules that fit well within a user-specified binding site of a receptor. The De Novo method is advantageous as it is fast and the variety of molecules that can be generated is extremely large. The protocol suggests how suitable fragments can be positioned into clefts of protein structures (for example active site of an enzyme) in such a way that hydrogen bonds can be formed with the enzyme and hydrophobic pockets are filled with hydrophobic groups. An advantage to this approach is that it is fast and a large number of fragments can be screened quickly. The protocol uses pre-generated AccelrysDS and ZINC libraries of str and trg files.

2.3.3 Fragment-based Lead Discovery

Fragment-based Lead Discovery is a new lead discovery approach that molecular weights are in the range of from 120 to 250Da comparing High Throughput Screening., screened molecular compounds are much lower in weight. Fragment-based hits are typically weak inhibitors in the range of 10 μ M to mM, hence need to be screened at higher concentration with sensitive detection techniques such as protein crystallography and NMR, rather than bioassays. Fragment-based fragments are simpler, less functionalized compounds with lower affinity. On the other hand, fragment hits typically possess high binding affinity per heavy atom called ligand efficiency. (RA, Congreve, Murray, & Rees, 2005)

In AccelrysDS we used De Nova Evolution protocol which uses a fragment based approach to suggest novel ligands from scaffold. Protocol adds small fragments from libraries to a scaffold in a protein active site. Fragments are placed in complementary positions to the receptor using a calculated interaction map to produce a collection of high scoring molecules. The nature of fragment selection and construction of new ligands depends on Evolution Mode. (Böhm, 1992) We used Full Evolution as the Evolution Mode of the protocol. In this mode, molecules are built in an evolutionary fashion starting from a scaffold and fragments are fused and then molecules are selected by score for the next iteration. LUDI scores are calculated as the scoring functions. We used FAST as the hit criteria that as soon as a hit has been found with a matching set of interaction sites, no further attempts are made to fit set of fragment target sites to any of the matched interaction.

2.3.4 Parameters and Scoring

We selected the radius of the input site sphere at the center of cavity, which defines a sphere in the receptor where receptor-ligands interactions are permitted. Fitting Scoring Function Ludi scoring function to use to prioritize the fragment hits for receptor-based runs. Ludi score is a sum of five contributions.

1. Contributions from ideal hydrogen bonds
2. Contributions from perturbed ionic interactions (donor/acceptor)
3. Contributions from lipophilic interactions
4. Contributions due to the freezing of internal degrees of freedom of the ligand
5. Contributions due to the loss of translational and rotational entropy of the ligand

Energy Estimate scoring functions are used for De Novo steps. They estimate the change in free energy upon binding the fragment to the receptor. Each fragment is evaluated as a function of the potential number of hydrogen bonding, hydrophobic and ionic contacts it can make and an estimate is made of the penalty due to freezing the internal degrees of freedom of the ligand. Fitting max Fit Attempts set to a 250. Fitting Maximum RMSD is set to 0.2\AA^0 . At each receptor, interaction site there is some range of interaction geometry between the ligand and receptor that maximizes the interaction. Deviation from this maximum, therefore, constitutes a measure of the quality of fit. Poor fits have high deviations and good fits have low deviations. As Ludi fits each fragment to the interaction sites, the RMSD is computed. From most fragments, if the RMSD exceeds the value of Maximum RMSD, the fragment is discarded. If Ludi is trying to fit a large fragment, it may allow the RMSD to exceed the value of the Maximum RMSD parameter. Number of replication, Fragment RMSD and Fragment partial charge method is set to 100, 0.2 and CHARMM respectively.

2.4 ADMET

ADMET is a set of test for human intestinal absorption (HIA). HIA is defined as a percentage absorbed rather than as a ratio of concentrations. A well-absorbed compound is one that is absorbed at least 90% into the bloodstream in humans. The intestinal absorption model in AccelrysDS includes 95% and 99% confidence ellipses in ADMET_PSA_2D, AlogP98 plane. The ellipses define regions where well-absorbed compounds should fall within the 99% ellipse. Note that the location of any particular compound does not necessarily imply whether it will be well, moderately, or poorly absorbed. Absorption drops off quite rapidly outside the 95% ellipse.

ADMET uses a few different models in the analysis. Aqueous solubility model uses linear regression to predict the solubility of each compound in water at 25⁰C. Blood Brain barrier model predicts blood-brain penetration using quantitative linear regression. Cytochrome P450 2D6 model predicts CYP2D6 enzyme inhibition using 2D chemical structure as input. Hepatotoxicity model predicts potential organ toxicity for a wide range of structurally diverse compounds. The plasma protein-binding model predicts whether a compound is likely to be highly bound to carrier proteins in the blood or not.

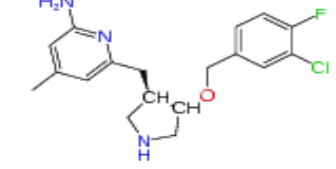
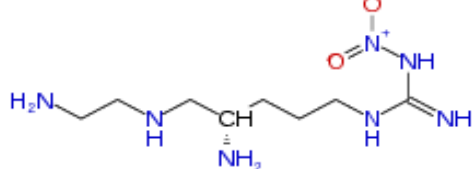
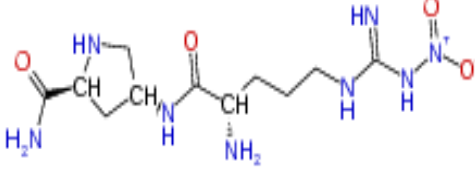
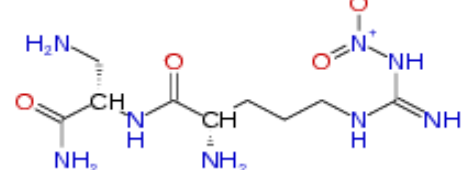
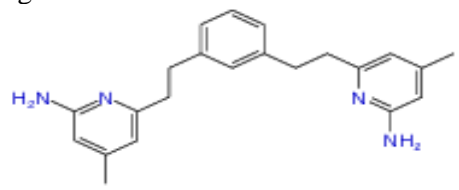
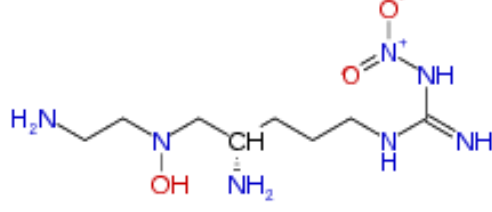
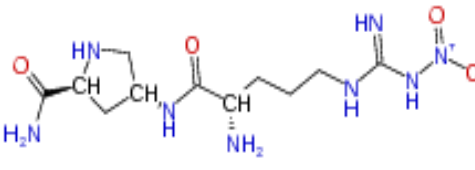
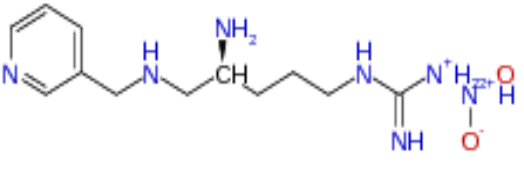
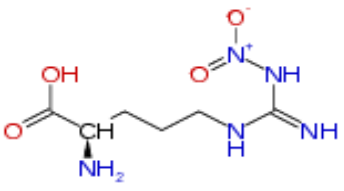
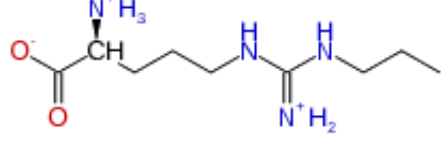
2.5 In silico VS In vitro Case

In the literature scanning, we accessed laboratory results for NOS enzymes studied in vitro. Here we tried to give a comparison to In silico. We have selected 24 articles containing selective inhibitor candidates from literature. We take the ligand-protein docking K_i values as the sample binding energy values and selected 16 compound to work on (Table 3).

We draw the ligand models from the scratch and minimized in AccelrysDS. To dock these ligands the enzyme files mentioned on the articles 3B3M, 3B3N, 3B3O, 3DQR, 3N2R and 3SVP nNOS receptors; 1FOI, 2NSE eNOS receptors; and 1NOD iNOS receptor are downloaded from the NCBI protein databank. We aimed to observe how the results changes in silico environments. 16 ligands group mostly having aromatic rings, fluorinated and chlorinated groups which are shown having effective in binding and guanidinium groups which have high cell membrane permeability. Energy minimizations were applied to these ligands by clean geometry and ligand optimization tools of AccelrysDS.

Enzymes decrease activation energies mainly in transition states. The transition state in a chemical reaction is a specific configuration on the reaction coordinate. The time step is typically at the femtosecond level and this step cannot be simulated. Instead, computational calculations based on highly improved force fields. Used AutoDock Free Energy Estimations are based on Van der Waals, Hydrogen bond, desolvation, Electrostatic, Torsional Free Energies and Unbound System Energy. Whereas in AccelrysDS scoring functions' contributions to evaluation is protein and amino acid related algorithms apart from force fields. LibDock is more concentrated on Hotspots like VDW and electrostatic attractions. For better binding, we are looking for lower AutoDock K_i values and higher CDocker and LibDock scores. In the field scoring functions used as fast approximation mathematical methods to predict the strength of the non-covalent interaction between two molecules after they have been docked.

We have chosen the 16 best ligands from the 24 different articles according to their experimental K_i values.

	Journal article reference and Ligand codes : ligand names and 2D conformation		Journal article reference and Ligand codes : ligand names and 2D conformation
1	(Silverman, et al., 2010) Lig1: 2k 	2	(Silverman,, et al., 2008) Lig2: ligand2 
3	(Silverman,, et al., 2008) Lig2_a : ligand3 	4	(Silverman, 2009) Lig3: L-ArgNO2-L-Dbu-NH2 
5	(Silverman, Poulos, Jamal, Li, Xue, & Delker, 2010) Lig4: 3h 	6	(Silverman, et al., 2007) Lig6: compound3 
7	(Silverman, Roman, Martasek, Gomez-Vidal, & Ji, 2006) Lig7: ligand 2d 	8	(Ji, Li, Flinspach, Poulos, & Silverman, 2003) Lig8: lig_III_2_CH2CH2NH2 
9	(Kowaluk, et al., 1998) Lig10: L-NNA 	10	(Zhang, Fast, Marletta, Martasek, & Silverman, 1997) Lig12: propyl 

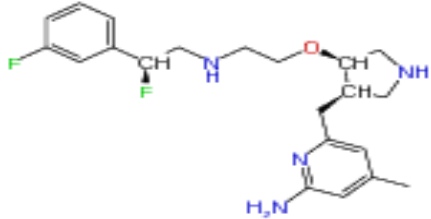
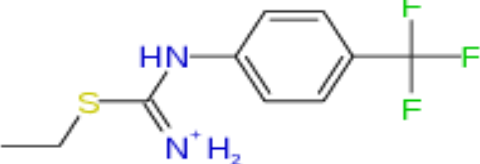
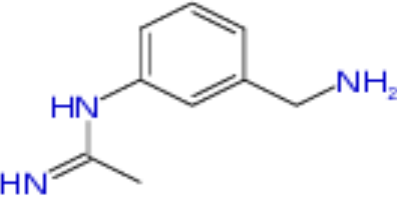
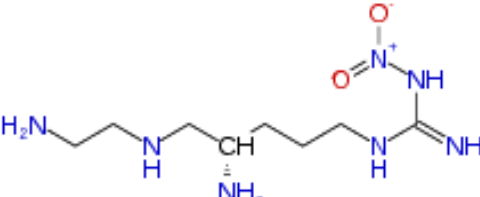
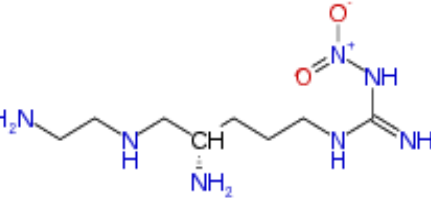
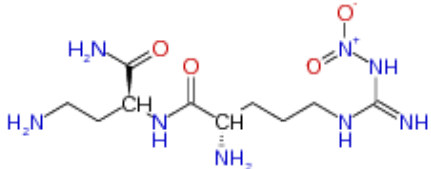
<p>11 (Fengtian, et al., 2011) Lig14: 8c</p> 	<p>12 (Lee, Oplinger, Frick, Garve, Furfine, & Shearer, 1997) Lig15: 39</p> 
<p>13 (Shearer, et al., 1998) Lig16: compound2</p> 	<p>14 (Hah, Martasek, Roman, & Silverman, 2003) Lig18 : RedAm-Ethyl (50)</p> 
<p>15 (Silverman, et al., 2007) Lig19: ligand1</p> 	<p>16 (Silverman, Martasek, Roman, Huang, & Hui, 2000) Lig20: L-ArgNO2-L-Dbu-NH2d</p> 

Table 3: 16 prominent selected ligands from recent NOS articles

We applied AutoDock docking to these 16 ligands using nNOS, eNOS and iNOS pdb files denoting the NOS enzyme in three groups. Then we compared the experimental values with the in silico values. According to log values we draw a line chart. In the line chart we have chosen closest line to the experimental value line. Among 5 closest nNOS protein we found 1RS7 is closest to experimental data for nNOS. 3DQS is selected as the same way to be used in the Lead De novo design as the enzyme frame. We had only one iNOS candidate so we used 1NSI directly.

2.6 Structural Alignment

Sequence analysis is frequently a first step in characterizing a potential protein target, because proteins with the same or similar functionality mostly share high sequence similarity. We used “Modeler Salign” function of AccelrysDS to structurally align macromolecular enzyme data records. It uses a general dynamic programming based alignment algorithm. The weight matrix used for dynamic programming is a weighted sum of five protein structure and sequence features: residue type, intermolecular distance of residue pairs, fractional side chains accessibility, secondary structure type and local conformation. At the end of alignments, different snapshots are taken from the 3D images. Additionally we used a Perl script on AccelrysDS named “BindingPocketSASAV2.pl” to display the cavity as a solvent accessible surface area and measure binding site volumes and visualize the positioning of the binding sites with the residues around.

3 Results

3.1 In silico vs. In vitro Case

In the literature there are laboratory results for NOS enzymes studied in vitro. We chose 16 ligands from 24 articles to define experimental ligand-protein docking K_i binding energy values. To dock these ligands we used 3B3M, 3B3N, 3B3O, 3DQR and 3N2R nNOS receptors; 1FOI, 3DQT and 3DQT eNOS receptors; and 1NSI iNOS receptor downloaded from the NCBI protein databank. We aimed to observe how the results changes in silico environments.

In the light of docking results of CDock, LibDock and AutoDock we decided to eliminate enzyme structures, which are not very compatible to our system. 1RS7 for nNOS and 3DQS for eNOS are set the foundation for the Lead discovery step. For iNOS, we did not have enough experimental data to test and compare in silico environment. Hence, we preferred to use 1NSI human enzyme which has a better resolution than 1NOD.

3.1.1 Docking Results for nNOS

AutoDock (nM)	Experimental Values	1RS7 (nNOS)	3B3N (nNOS)	3B3O (nNOS)	3DQR (nNOS)	3N2R (nNOS)
lig1	760.00	321.20	162.22	192.87	152.86	60.87
lig2	120.00	209.45	905.57	964.70	1030.00	265.79
ig2_a	100.00	32.63	5.97	16.86	145.30	10.61
lig3	130.00	393.07	439.24	1000.00	406.00	249.02
lig4	38.00	578.73	327.46	213.90	420.61	99.25
lig6	120.00	2160.00	611.71	1370.00	210.79	603.38
lig7	100.00	98.03	222.36	53.19	136.84	37.99
lig8	50.00	89.14	269.51	573.45	855.42	134.67
lig10	600.00	1260.00	13310.00	3220.00	932.65	2810.00
lig12	57.00	571.16	1440.00	1810.00	2150.00	765.08
lig14	26.00	7090.00	366.09	263.80	4640.00	823.77
lig15	320.00	32030.00	49310.00	45800.00	27700.00	43720.00
lig16	15.00	9820.00	8080.00	11510.00	22710.00	8310.00
lig18	120.00	349.84	472.66	369.78	619.01	171.04
lig19	170.00	472.13	703.23	612.95	1010.00	171.97
lig20	130.00	404.40	1040.00	374.36	1530.00	652.15

Table 4: *AutoDock* results of 16 prominent ligands on 5 different nNOS crystal structures

ADock Log(nM)	Experimental Values	1RS7 (nNOS)	3B3N (nNOS)	3B3O (nNOS)	3DQR (nNOS)	3N2R (nNOS)
lig1	2.88	2.51	2.21	2.29	2.18	1.78
lig2	2.08	2.32	2.96	2.98	3.01	2.42
ig2_a	2.00	1.51	0.78	1.23	2.16	1.03
lig3	2.11	2.59	2.64	3.00	2.61	2.40
lig4	1.58	2.76	2.52	2.33	2.62	2.00
lig6	2.08	3.33	2.79	3.14	2.32	2.78
lig7	2.00	1.99	2.35	1.73	2.14	1.58
lig8	1.70	1.95	2.43	2.76	2.93	2.13
lig10	2.78	3.10	4.12	3.51	2.97	3.45
lig12	1.76	2.76	3.16	3.26	3.33	2.88
lig14	1.41	3.85	2.56	2.42	3.67	2.92
lig15	2.51	4.51	4.69	4.66	4.44	4.64
lig16	1.18	3.99	3.91	4.06	4.36	3.92
lig18	2.08	2.54	2.67	2.57	2.79	2.23
lig19	2.23	2.67	2.85	2.79	3.00	2.24
lig20	2.11	2.61	3.02	2.57	3.18	2.81

Table 5: *Log* values of *AutoDock* Results of Table 4

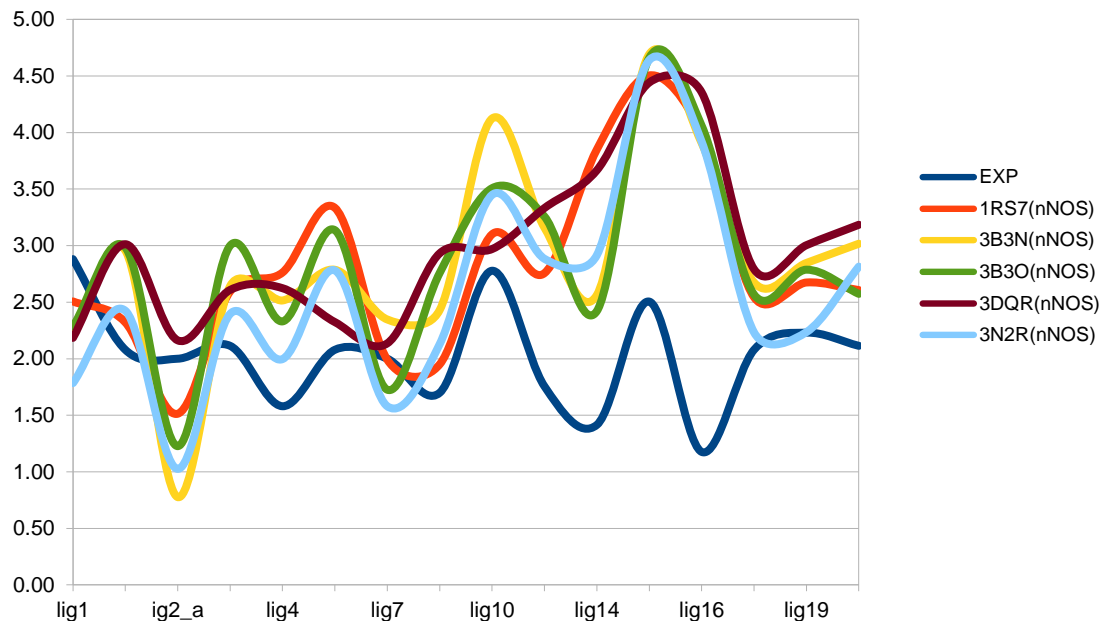


Figure 11: nNOS AutoDock results chart of Table 5 denoting logarithmic behavior of inhibition constants

C-DOCK	1RS7 (nNOS)	3B3N (nNOS)	3B30 (nNOS)	3DQR (nNOS)	3N2R (nNOS)
lig1	22.79	28.89	14.35	26.83	x
lig2	45.35	46.83	30.80	43.36	x
lig2_a	33.18	37.78	16.23	38.53	x
lig3	52.21	56.27	34.83	50.85	x
lig4	50.07	48.54	44.65	49.47	x
lig6	40.20	42.27	27.07	39.32	x
lig7	38.00	33.76	19.77	31.47	x
lig8	x	x	x	x	x
lig10	35.37	36.26	23.00	36.38	35.44
lig12	52.17	65.09	43.72	57.10	66.06
lig14	30.96	30.73	29.28	18.12	27.24
lig15	18.33	23.61	9.36	18.44	23.41
lig16	23.29	27.35	16.59	22.94	24.61
lig18	43.70	44.61	28.78	39.19	45.09
lig19	43.19	44.88	30.86	41.09	44.35
lig20	51.10	54.67	39.04	53.54	53.40

Table 6: C-Dock results of 16 prominent ligands on 5 different nNOS crystal structures

LIBDOCK	1RS7 (nNOS)	3B3N (nNOS)	3B30 (nNOS)	3DQR (nNOS)	3N2R (nNOS)
lig1	157.97	143.46	127.73	138.64	131.14
lig2	107.50	113.73	77.64	112.33	113.04
lig2_a	127.88	136.71	117.22	129.25	137.50
lig3	134.10	133.39	87.39	133.95	138.15
lig4	156.34	161.48	134.96	150.92	158.50
lig6	122.19	119.64	x	116.32	116.70
lig7	138.11	143.40	137.53	144.54	144.72
lig8	113.03	111.23	110.94	115.55	111.26
lig10	104.96	105.04	77.12	103.09	101.23
lig12	110.19	114.21	90.44	107.94	110.13
lig14	156.29	156.71	149.85	151.63	158.16
lig15	92.94	97.20	95.09	93.05	89.37
lig16	96.00	92.57	99.32	97.72	94.04
lig18	110.31	108.96	88.73	117.62	109.90
lig19	107.50	113.73	77.64	112.33	113.04
lig20	135.26	138.39	107.01	131.25	142.54

Table 7: LibDock results of 16 prominent ligands on 5 different nNOS crystal structure

According to the docking result above, we have eliminated all others but the 1RS7 protein file, which satisfied the closest in silico results comparing to in vitro results. We proceed to the next step which is Lead Discovery by these nNOS enzymes.

3.1.2 Docking Results for eNOS

AutoDock (nM)	Experimental Values	1FOI (eNOS)	3DQS (eNOS)	3DQT (eNOS)
lig1	13300	822.72	661.69	579.00
lig2	314000	119.45	736.55	1.32
ig2_a	128000	32.75	11.48	1.93
lig3	200000	718.31	701.88	2.49
lig4	4200	360.21	291.57	1030.00
lig6	73000	180.07	4600.00	1.94
lig7	128000	26.76	174.50	0.17
lig8	105000	34.44	170.85	0.73
lig10	1200	54.07	1930.00	0.10
lig12	8500	26.72	2240.00	0.28
lig14	19000	1470.00	551.51	1940.00
lig15	9400	45790.00	78250.00	61780.00
lig16	30	7980.00	5490.00	7640.00
lig18	314000	16.72	624.81	1.97
lig19	191000	82.56	3070.00	0.55
lig20	2000000	173.48	1730.00	1.21

Table 8: *AutoDock* results of 16 prominent ligands on five different eNOS crystal structures

ADock Log(nM)	Experimental Values	1FOI (eNOS)	3DQS (eNOS)	3DQT (eNOS)
lig1	4.12	2.92	2.82	2.76
lig2	5.50	2.08	2.87	0.12
ig2_a	5.11	1.52	1.06	0.29
lig3	5.30	2.86	2.85	0.40
lig4	3.62	2.56	2.46	3.01
lig6	4.86	2.26	3.66	0.29
lig7	5.11	1.43	2.24	-0.77
lig8	5.02	1.54	2.23	-0.14
lig10	3.08	1.73	3.29	-1.02
lig12	3.93	1.43	3.35	-0.55
lig14	4.28	3.17	2.74	3.29
lig15	3.97	4.66	4.89	4.79
lig16	1.48	3.90	3.74	3.88
lig18	5.50	1.22	2.80	0.29
lig19	5.28	1.92	3.49	-0.26
lig20	6.30	2.24	3.24	0.08

Table 9: *Log* values of *AutoDock* Results of Table 8

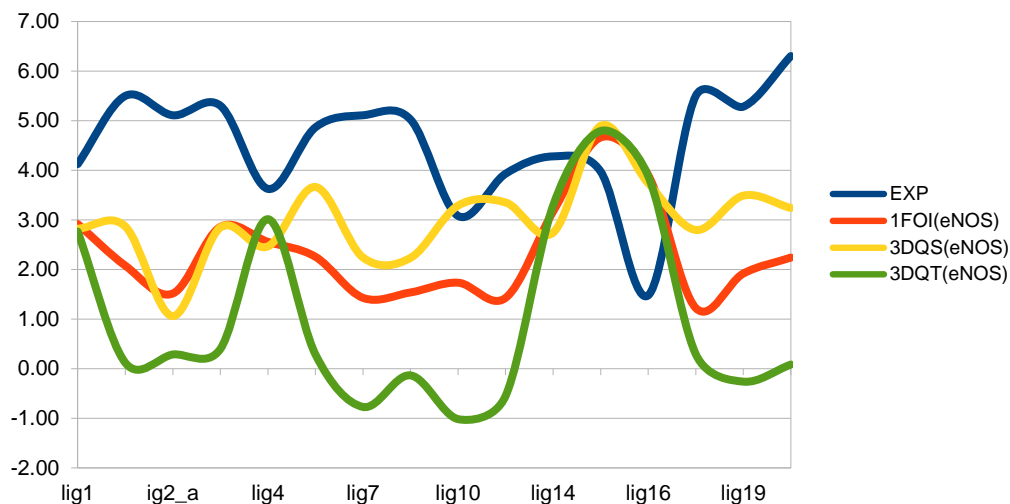


Figure 12 : eNOS AutoDock results chart of Table 9. denoting logarithmic behavior of inhibition constants

C-DOCK	1FOI (eNOS)	3DQS (eNOS)	3DQT (ENOS)	1NSI (iNOS)
lig1	19.93	21.21	-4.71	24.14
lig2	44.00	42.81	34.89	44.36
lig2_a	33.54	30.84	12.29	38.20
lig3	42.15	49.92	39.91	61.54
lig4	45.67	50.85	26.41	52.25
lig6	38.04	37.92	31.34	51.08
lig7	40.07	31.41	8.59	40.71
lig8	x	x	x	x
lig10	37.31	35.87	26.91	44.27
lig12	67.50	62.92	39.16	81.75
lig14	26.61	29.60	20.59	28.72
lig15	16.49	16.29	11.35	23.60
lig16	19.22	19.13	17.20	27.12
lig18	40.86	37.76	33.63	44.80
lig19	39.52	38.18	36.70	48.96
lig20	50.06	53.07	26.65	60.18

Table 10: C-Dock results of 16 prominent ligands on 5 different eNOS crystal structures

LIBDOCK	1FOI (eNOS)	3DQS (eNOS)	3DQT (eNOS)	1NSI (iNOS)
lig1	141.05	146.02	129.00	137.19
lig2	106.42	110.54	106.14	102.88
lig2_a	120.68	124.88	62.05	132.76
lig3	127.61	114.60	115.34	130.10
lig4	155.69	157.33	141.51	153.76
lig6	119.66	106.54	114.42	105.23
lig7	128.83	134.89	98.94	137.91
lig8	102.26	118.58	x	107.87
lig10	102.81	98.41	89.11	103.83
lig12	109.90	102.85	99.31	101.78
lig14	144.82	148.67	143.30	141.98
lig15	84.14	86.10	78.64	84.20
lig16	96.24	92.24	82.03	92.94
lig18	100.23	94.85	88.26	97.15
lig19	108.55	110.54	106.14	102.87
lig20	143.16	132.70	142.84	123.19

Table 11: *LibDock* results of 16 prominent ligands on 5 different eNOS crystal structures

According to the docking result above, we chose the 3DQS protein file, which yields the closest in silico results comparing to in vitro results. We proceed to the next step, which is Lead Discovery by this eNOS enzyme.

3.2 De Novo Results

3.2.1 Lead Discovery Results

From the AccelrysDS and ZINC libraries, we filtered out 6 molecules on 1RS7 nNOS, 2 molecules on 3DQS eNOS and, 2 molecules on 1NSI iNOS scaffolds from more than a million lead according to the Ludi scores. These 9 leads are going to be scaffolds in fragment-based lead discovery stage. De Novo best lead discovery results are shown in Table 12

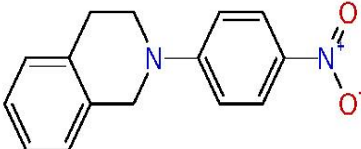
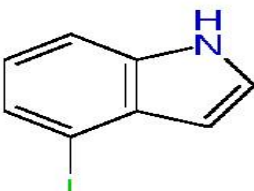
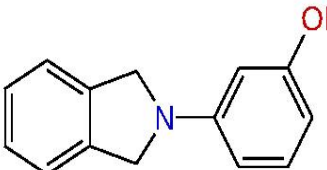
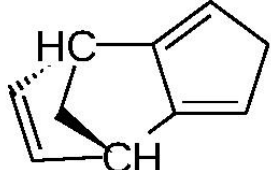
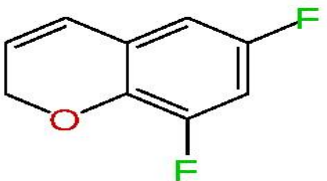
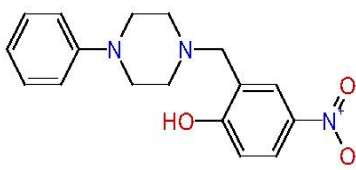
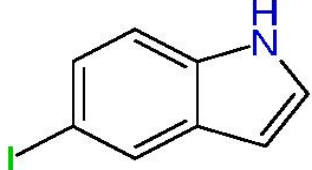
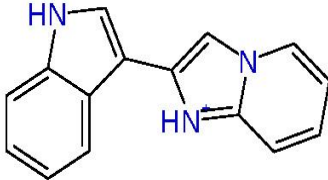
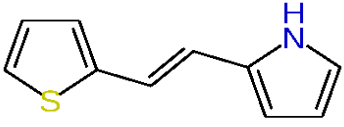
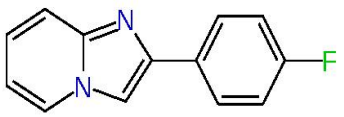
ZINC Lib. Molecule Ludi Score	Structure	ZINC Lib. Molecule Ludi Score	Structure
P_0_3 zinc04859564 885 3RS7 - nNOS		P_0_5 zinc42689701 779 3RS7 - nNOS	
P_0_5 zinc00056346 861 3RS7 - nNOS		P_0_8 zinc71786250 832 3RS7 - nNOS	
P_0_9 zinc39941619 816 3RS7 - nNOS		P_1_1 zinc35335410 741 3RS7 - nNOS	
P_0_9_0_80_7 zinc00081090 900 3DQS - eNOS		P_1_1 zinc12546533 711 3DQS - eNOS	
P_0_9_0_80_7 zinc04649158 575 1NSI - iNOS		P_1_1 zinc00151524 766 1NSI - iNOS	

Table 12: De Novo Lead Discovery (best ZINC molecules that will be used as a Lead in the Fragment based De Novo Stage)

3.2.2 De Novo Fragment Based Discovery Results

Each new leads are developed in fragments libraries and best 10 of evolved molecules are docked back to NOS enzymes. Total 100 evolved molecules are docked back to main three NOS isozymes. From the docking result in Table 14, we have selected the evolved 17 molecules (Table 13) whose AutoDock Ki values and CDock Ludi Scores reveal selectivity in binding. Best fragment based discovery results are given in Table 13

Ludi Score MWeight	Structure	Ludi Sc. MWeight	Structure
1NSI_zinc00151524			
Evo3 1266 542		Evo6 1246 584	
Evo7 1230 548		Evo10 1222 541	
1NSI_zinc04649158			
Evo2 1054 529		Evo3 1053 574	
Evo4 1048 514			
1RS7_zinc39941619			

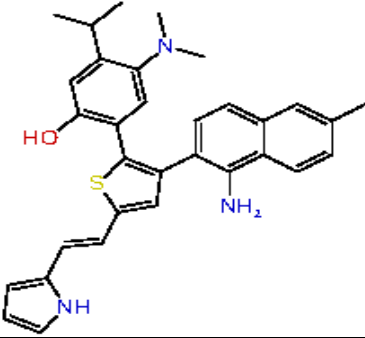
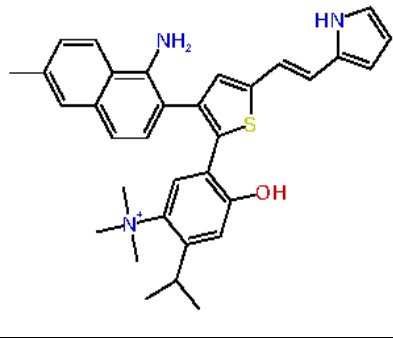
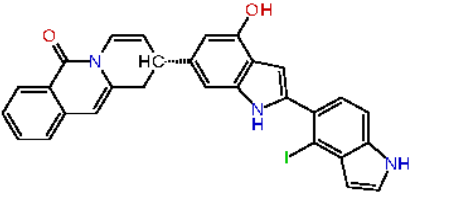
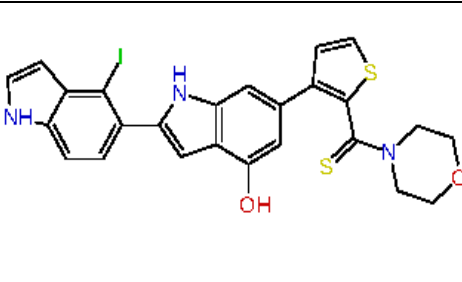
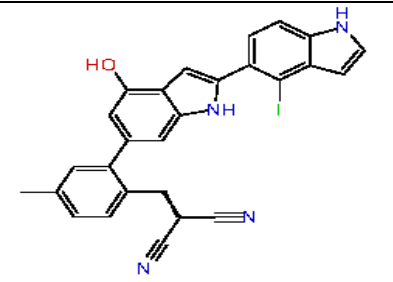
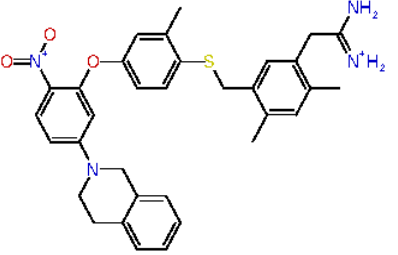
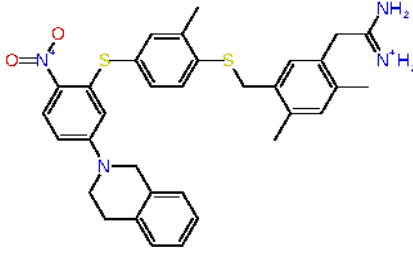
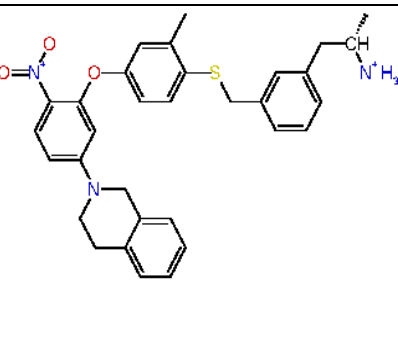
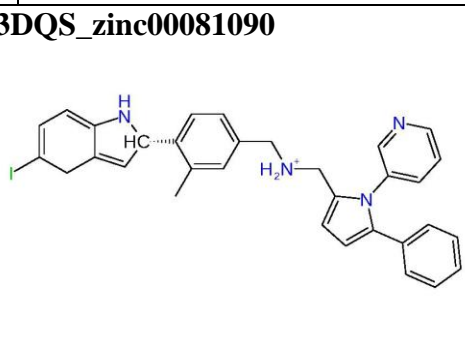
Evo9 1017 508		Evo10 1017 523	
1RS7_zinc42689701			
Evo5 1378 569			
Evo6 1375 585		Evo10 1351 540	
1RS7_zinc04859564			
Evo5 1253 568		Evo6 1246 584	
Evo10 1222 541		Evo_8 1444 524	3DQS_zinc00081090 

Table 13 Fragment Based Discovery drug candidates and their, Ludi Scores and

3.3 ADMET Results

The ADMET behaviors of the selected evolved drug candidate molecules shown in Figure 13 states that five of them are not suitable for HIA. ADMET failing compounds are 1NSI_zinc00151524_evo6, 1NSI_zinc04649158_evo2, evo3 and evo4 and 1RS7_zinc04859564_evo9,evo10. The others, all fall into the middle of the area enclosed by ADMET boundary eclipses denoting they are better candidates to be a drug. In Figure 13, a few of the enzymes overlap in the same points denoted by blue color.

“1NSI_zinc00151524_Evo3,Evo7, Evo10 “, “1RS7_zinc42689701_Evo5, Evo 6, Evo 10”, “1RS7_zinc04859564_Evo5, Evo 6, Evo 10” and “3DQS_zinc00081090_Evo8” are all have outstanding ADMET results.

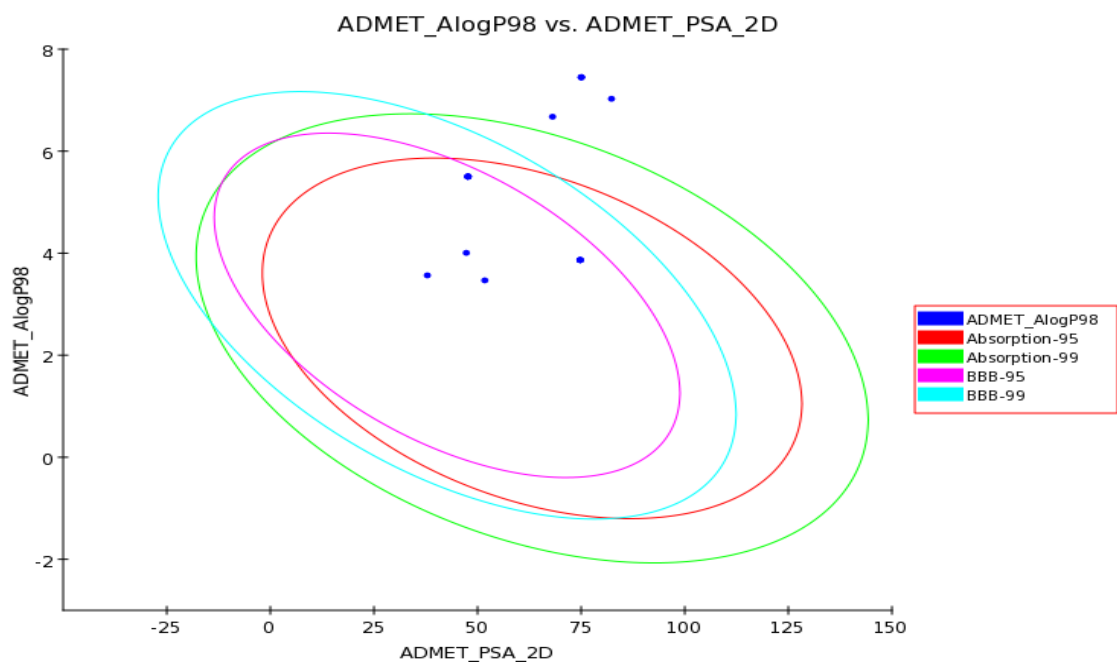


Figure 13: ADMET results of molecules evolved in fragment De Novo

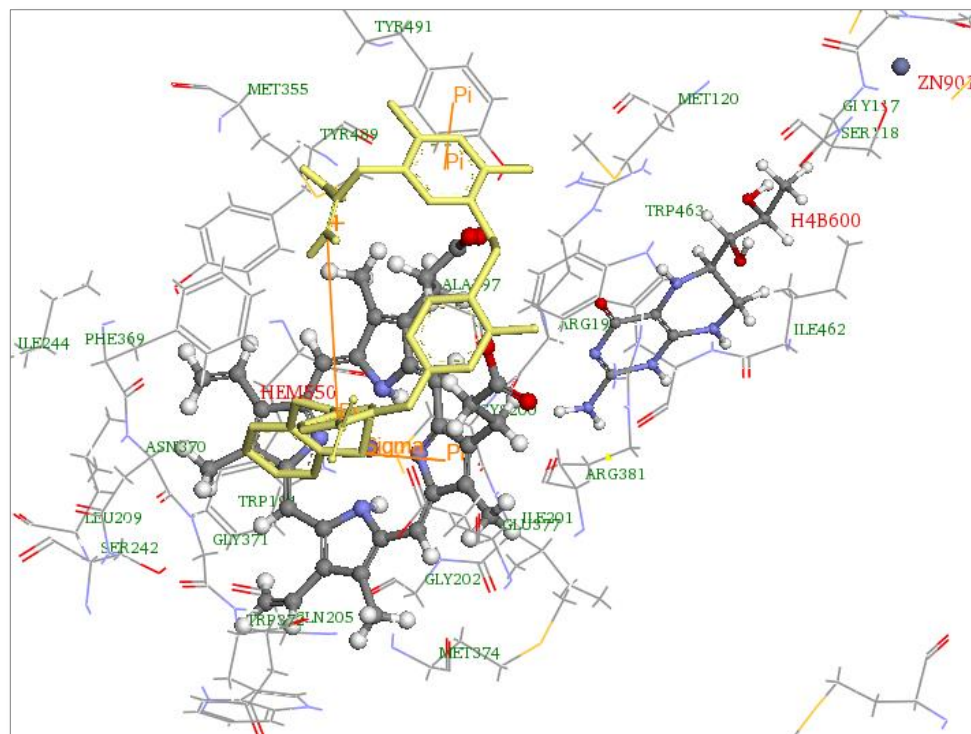
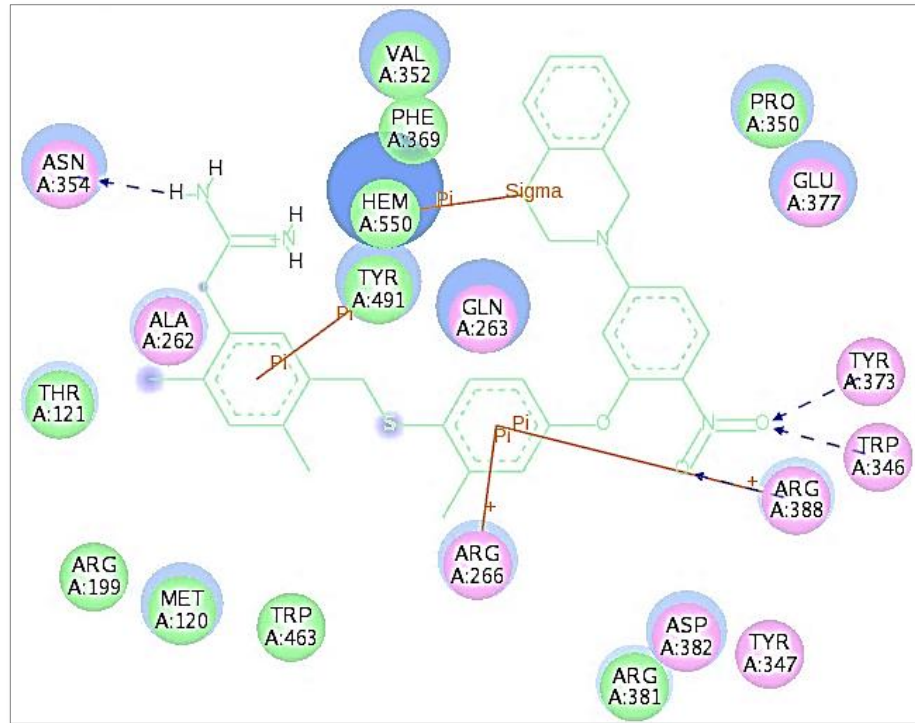


Figure 15: 2D&3D images of INSI and zinc00151524_evo7 interaction

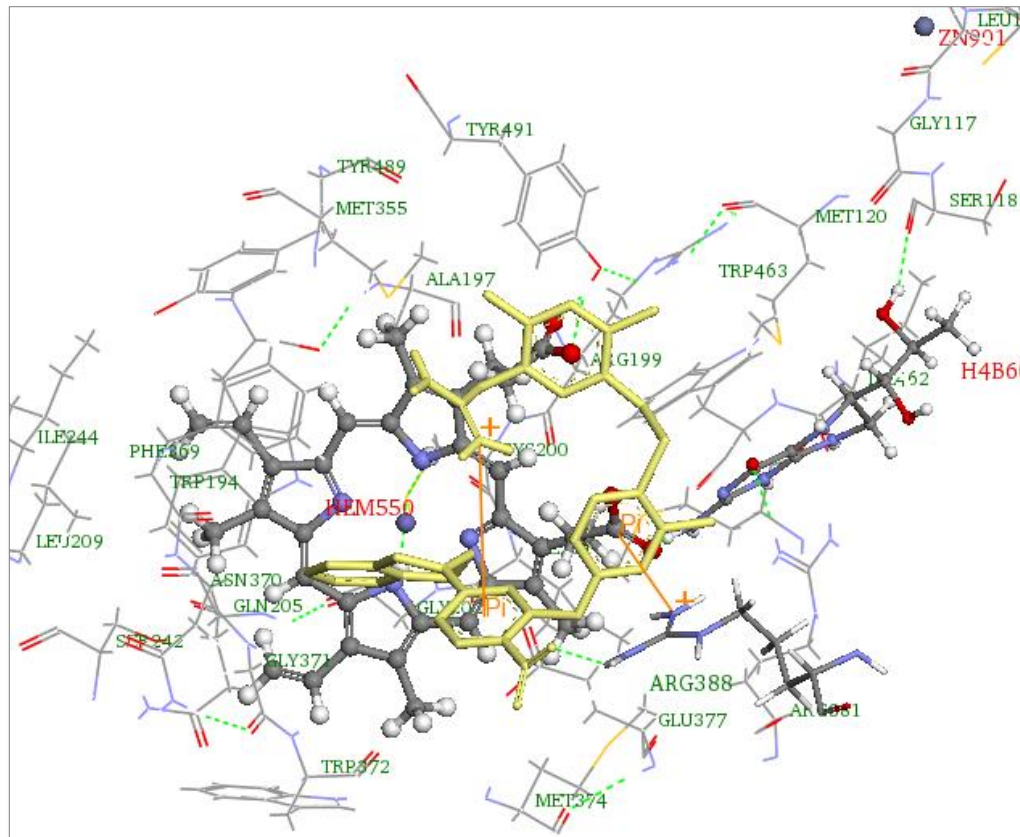
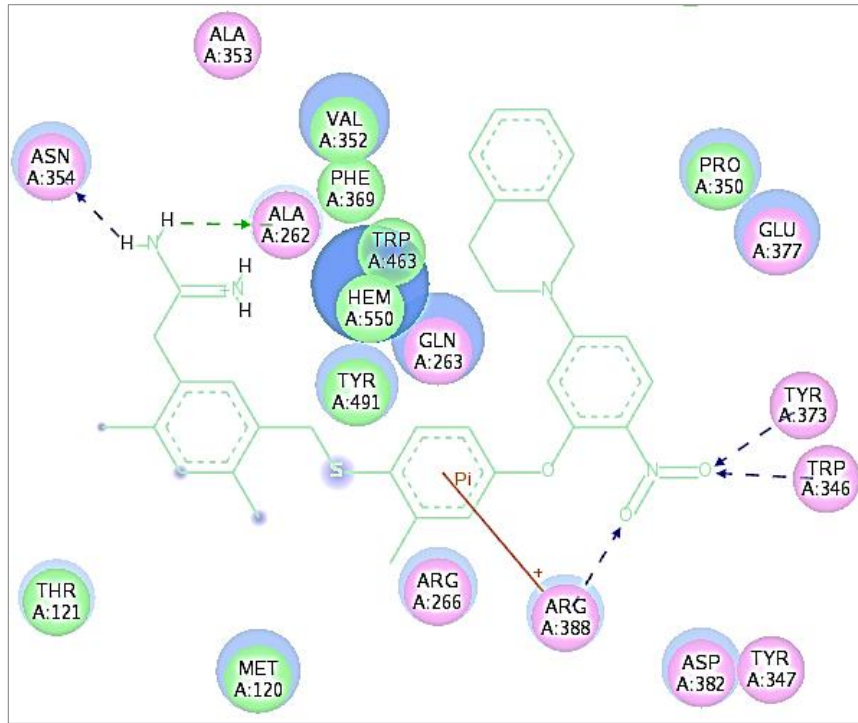


Figure 16: 2D&3D images of INSI and zinc00151524_evo10 interaction

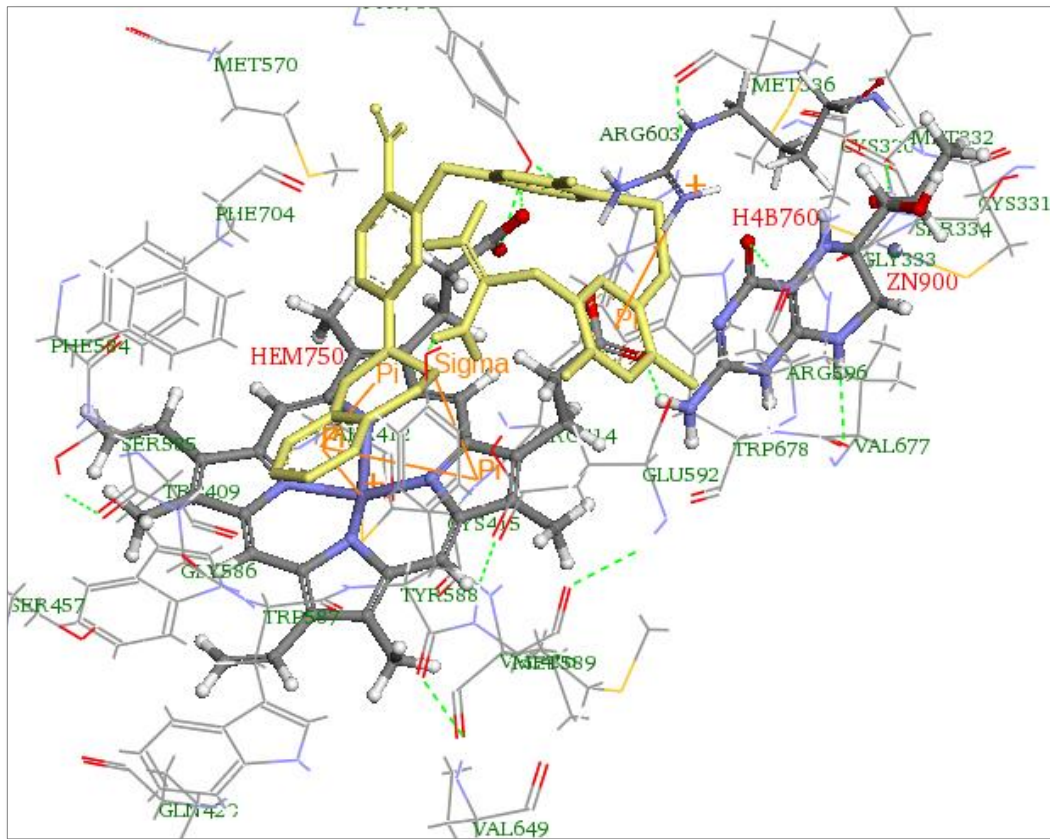
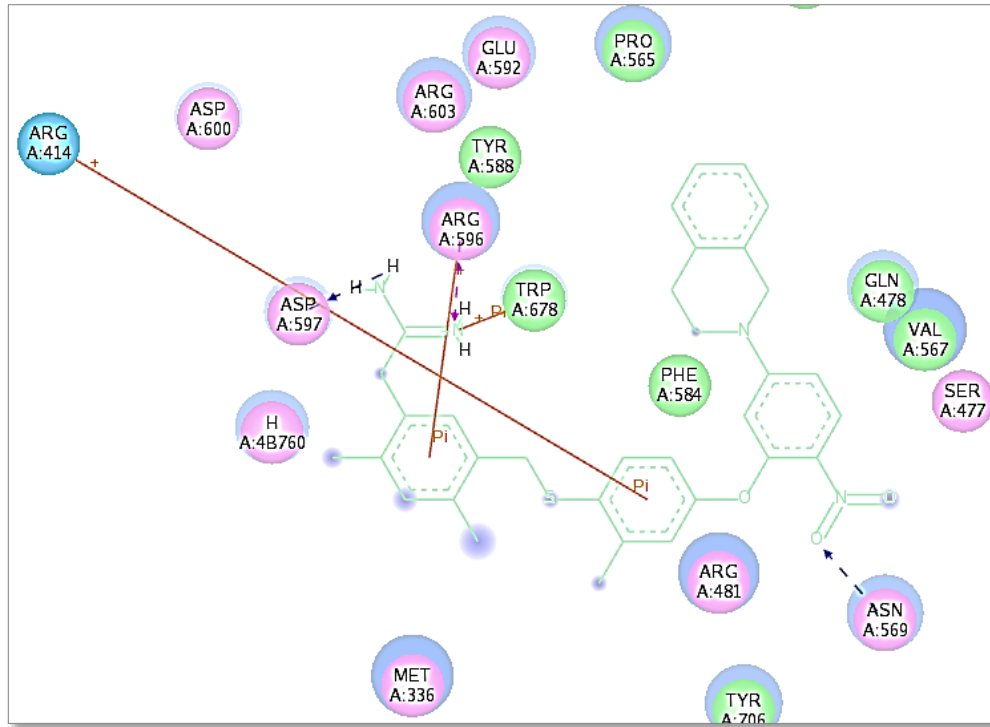


Figure 17: 2D&3D images of IRS7 and IRS7_zinc04859564_evo5

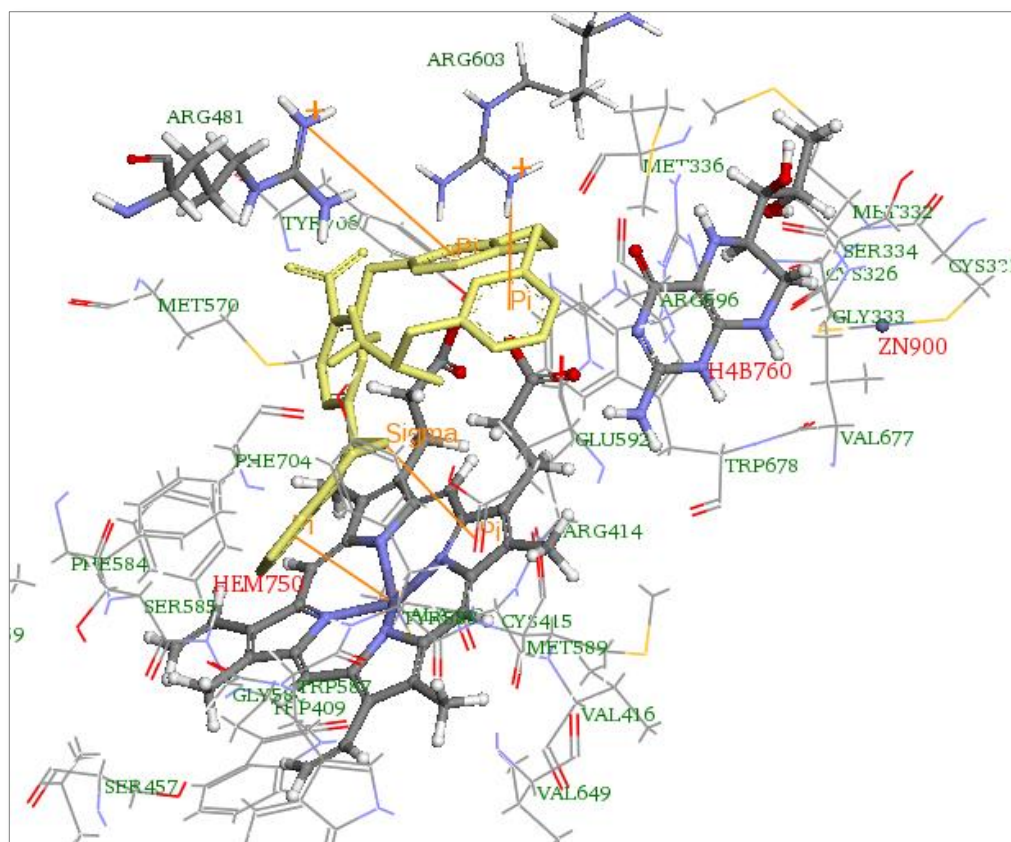
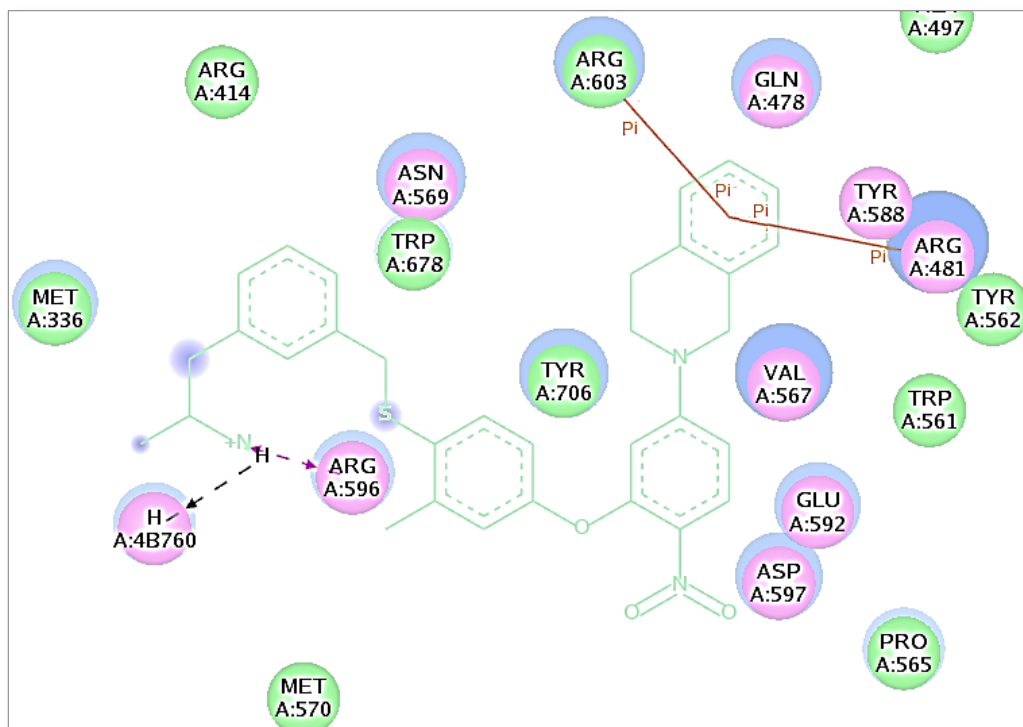


Figure 19 : 2D&3D images of IRS7 and IRS7_zinc04859564_evo10 interaction

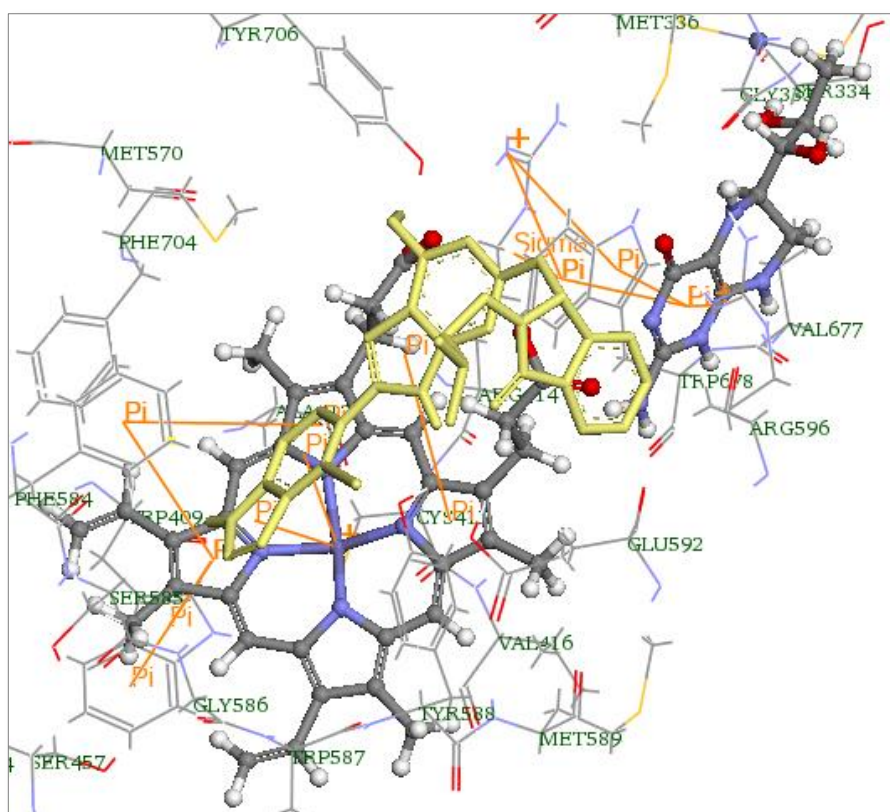
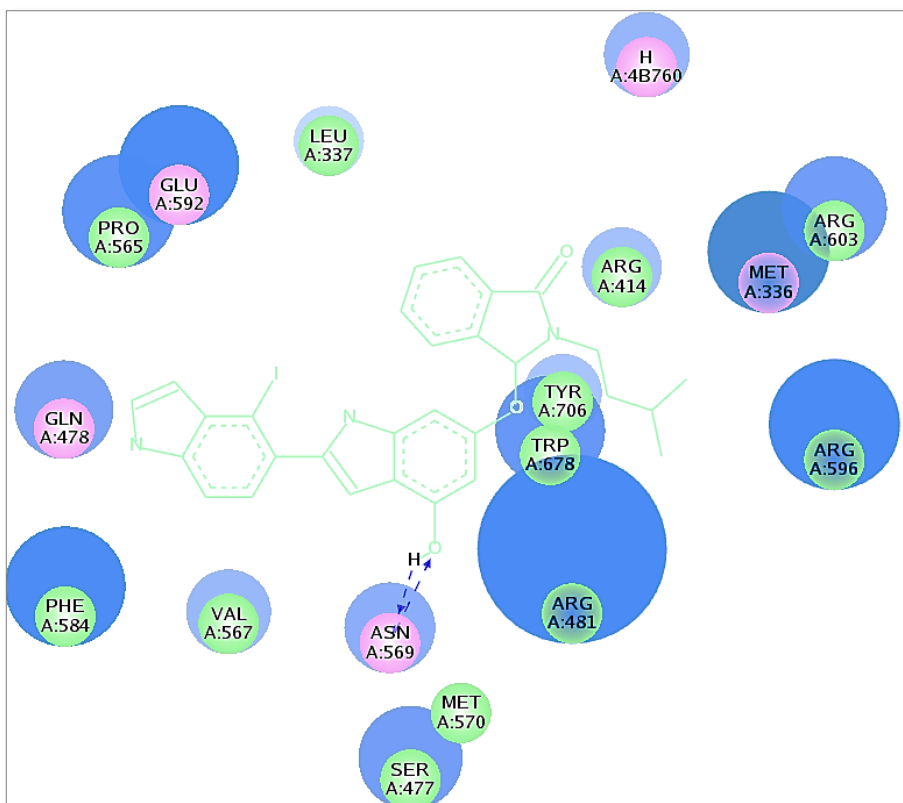


Figure 20: 2D&3D images of IRS7 and IRS7_zinc42689701_evo5 interaction

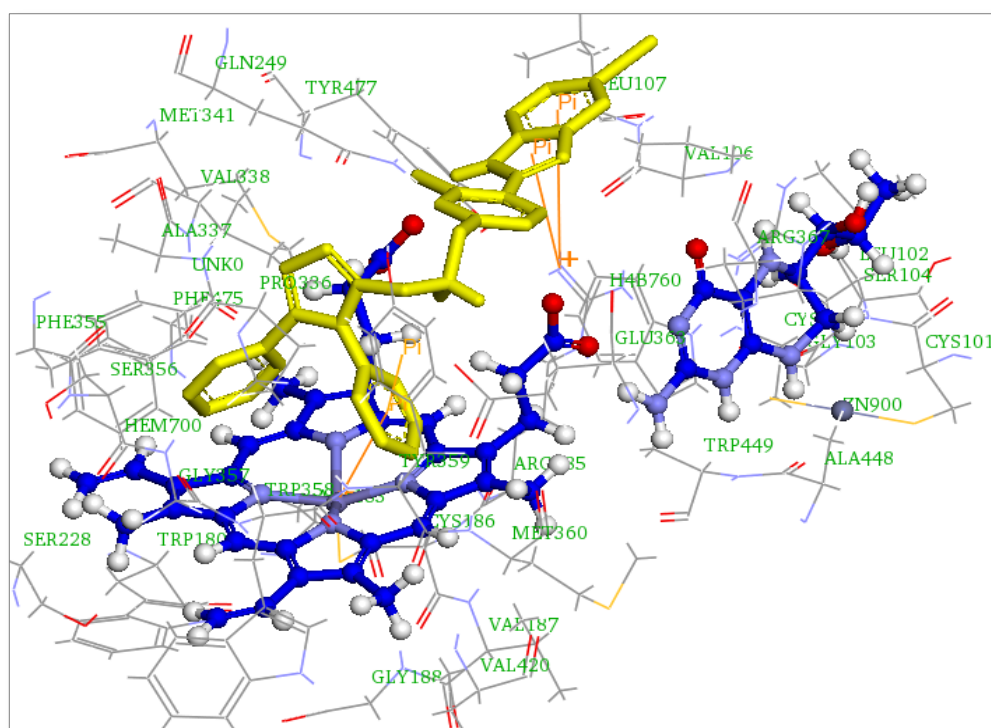
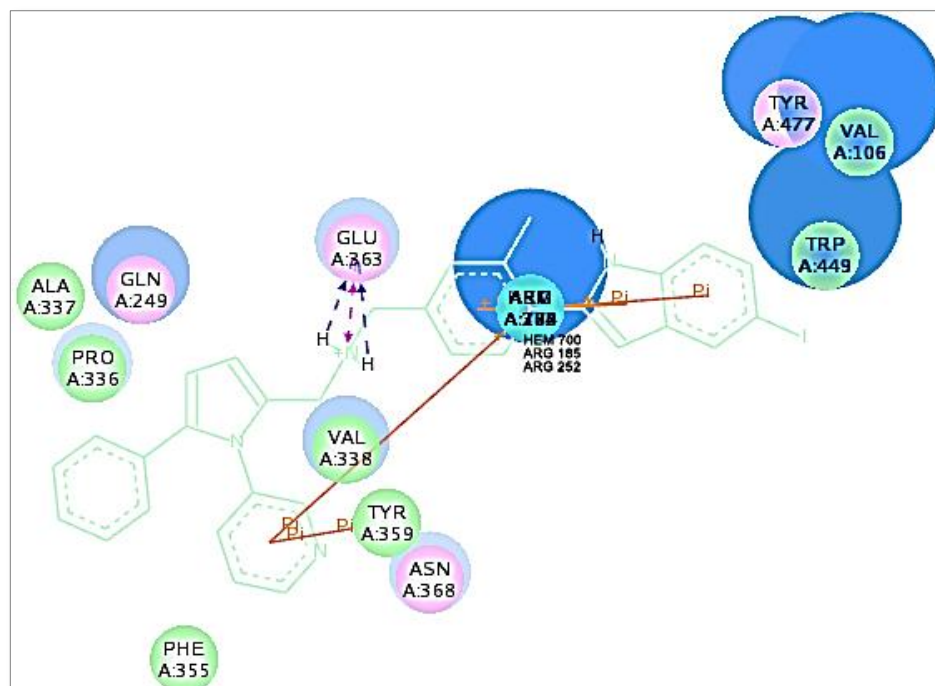


Figure 23: 2D&3D images of 3DQS and 3DQS_zinc00081090_Evo8 interaction

Ligands	AutoDocks (All Ki values in nm)							LibDocks Scores		
	1NSI	1RS7	3DQS				1NSI	1RS7	3DQS	
	iNOS	nNOS	eNOS	n/e	n/i	e/n	i/n	iNOS	nNOS	eNOS
1NSI_zinc00151524_evo1	63.96	4.6	10.53	0.4	0.1	2.3	13.9	52.96	154.76	132.26
1NSI_zinc00151524_evo2	75.17	4.25	3.64	1.2	0.1	0.9	17.7	57.65	125.02	116.01
1NSI_zinc00151524_evo3	94.75	2.72	28.97	0.1	0.0	10.7	34.8	x	117.27	76.02
1NSI_zinc00151524_evo4	72.36	3.96	14.53	0.3	0.1	3.7	18.3	x	87.81	69.17
1NSI_zinc00151524_evo5	103.38	59.15	365.18	0.2	0.6	6.2	1.7	x	147.39	119.60
1NSI_zinc00151524_evo6	585	12.9	332.05	0.0	0.0	25.7	45.3	x	127.14	113.65
1NSI_zinc00151524_evo7	345.43	6.28	716.13	0.0	0.0	114.0	55.0	x	113.52	73.49
1NSI_zinc00151524_evo8	974.44	71.26	364.63	0.2	0.1	5.1	13.7	x	96.61	92.16
1NSI_zinc00151524_evo9	368.15	59.37	426.26	0.1	0.2	7.2	6.2	x	113.86	89.53
1NSI_zinc00151524_evo10	123.06	3.49	194.76	0.0	0.0	55.8	35.3	x	127.49	88.97
AutoDocks	1NSI	1RS7	3DQS				1NSI	1RS7	3DQS	
	iNOS	nNOS	eNOS	n/e	n/i	e/n	i/n	iNOS	nNOS	eNOS
1NSI_zinc04649158_evo1	9700	3.76	11.66	0.3	0.0	3.1	2579.8	x	135.41	123.30

1NSI_zinc04649158_evo2	95.52	0.44088	124.2	0.0	0.0	281.7	216.7	x	138.34	123.71
1NSI_zinc04649158_evo3	93.95	0.53878	131.48	0.0	0.0	244.0	174.4	x	x	139.59
1NSI_zinc04649158_evo4	93.74	0.35568	152.75	0.0	0.0	429.5	263.6	x	134.58	121.28
1NSI_zinc04649158_evo5	7.2	0.46604	2.18	0.2	0.1	4.7	15.4	x	144.58	124.41
1NSI_zinc04649158_evo6	13.34	0.45125	1.24	0.4	0.0	2.7	29.6	x	148.28	131.03
1NSI_zinc04649158_evo7	11.6	0.41526	1.49	0.3	0.0	3.6	27.9	x	149.52	145.30
1NSI_zinc04649158_evo8	7.67	0.76733	2.15	0.4	0.1	2.8	10.0	x	146.15	134.86
1NSI_zinc04649158_evo9	7.95	0.46691	1.77	0.3	0.1	3.8	17.0	x	x	66.50
1NSI_zinc04649158_evo10	42.58	103.38	626.49	0.2	2.4	6.1	0.4	x	125.61	56.74

	1NSI	1RS7	3DQS						1NSI	1RS7	3DQS
AutoDocks	iNOS	nNOS	eNOS	n/e	n/i	e/n	i/n		iNOS	nNOS	eNOS
1RS7_zinc00056346_evo1	11	1.5	14.75	0.1	0.1	9.8	7.3	x	168.68	120.99	
1RS7_zinc00056346_evo2	3.08	2.35	14.47	0.2	0.8	6.2	1.3	x	165.51	117.68	
1RS7_zinc00056346_evo3	5.26	2.02	5.17	0.4	0.4	2.6	2.6	x	164.49	117.41	
1RS7_zinc00056346_evo4	2.87	1.88	10.56	0.2	0.7	5.6	1.5	x	163.26	112.87	
1RS7_zinc00056346_evo5	5.01	2.98	19.65	0.2	0.6	6.6	1.7	x	162.35	116.39	
1RS7_zinc00056346_evo6	5.79	1.67	3.57	0.5	0.3	2.1	3.5	x	160.44	124.37	
1RS7_zinc00056346_evo7	4.01	1.68	5.44	0.3	0.4	3.2	2.4	122.18	148.60	130.92	

1RS7_zinc00056346_evo8	6.23	2.13	7.34	0.3	0.3	3.4	2.9	118.98	160.35	135.28
1RS7_zinc00056346_evo9	3.26	1.79	8.57	0.2	0.5	4.8	1.8	x	149.67	131.39
1RS7_zinc00056346_evo10	3.79	8.72	19.46	0.4	2.3	2.2	0.4	129.20	151.20	132.38

	1NSI	1RS7	3DQS					1NSI	1RS7	3DQS
AutoDocks	iNOS	nNOS	eNOS	n/e	n/i	e/n	i/n	iNOS	nNOS	eNOS

1RS7_zinc39941619_Evo_1	1.79	3.49	2.15	1.6	1.9	0.6	0.5	x	137.56	143.36
1RS7_zinc39941619_Evo_2	0.10248	17.91	41.04	0.4	174.8	2.3	0.0	x	148.49	136.36
1RS7_zinc39941619_Evo_3	0.11523	2.62	4.28	0.6	22.7	1.6	0.0	x	115.78	126.48
1RS7_zinc39941619_Evo_4	4120	10.69	97.63	0.1	0.0	9.1	385.4	x	114.35	126.55
1RS7_zinc39941619_Evo_5	4120	11.3	91.7	0.1	0.0	8.1	364.6	x	135.61	135.03
1RS7_zinc39941619_Evo_6	4280	9.94	118.73	0.1	0.0	11.9	430.6	x	126.20	98.39
1RS7_zinc39941619_Evo_7	4110	9.86	101.08	0.1	0.0	10.3	416.8	x	153.60	108.24
1RS7_zinc39941619_Evo_8	58220	100.05	869	0.1	0.0	8.7	581.9	x	x	116.98

1RS7_zinc39941619_Evo_9	112860	137.65	10260	0.0	0.0	74.5	819.9	x	154.09	96.58
1RS7_zinc39941619_Evo_10	71710	146.13	68660	0.0	0.0	469.9	490.7	x	139.95	82.28

	1NSI	1RS7	3DQS					1NSI	1RS7	3DQS
AutoDocks	iNOS	nNOS	eNOS	n/e	n/i	e/n	i/n	iNOS	nNOS	eNOS

1RS7_zinc42689701_Evo_1	576.36	33.89	81.55	0.4	0.1	2.4	17.0	141.15	128.66	119.72
-------------------------	--------	-------	-------	-----	-----	-----	------	--------	--------	--------

1RS7_zinc42689701_Evo_2	2520	30.32	2080	0.0	0.0	68.6	83.1	x	120.72	114.35
1RS7_zinc42689701_Evo_3	2510	34.47	2050	0.0	0.0	59.5	72.8	124.78	133.69	116.86
1RS7_zinc42689701_Evo_4	383.81	40.32	306.67	0.1	0.1	7.6	9.5	122.84	133.56	111.65
1RS7_zinc42689701_Evo_5	354.01	16.65	252.47	0.1	0.0	15.2	21.3	x	141.21	139.58
1RS7_zinc42689701_Evo_6	404.46	12.27	251.22	0.0	0.0	20.5	33.0	111.83	123.16	103.43
1RS7_zinc42689701_Evo_7	379.74	17.75	339.9	0.1	0.0	19.1	21.4	117.57	137.11	137.56
1RS7_zinc42689701_Evo_8	379.6	45.6	1200	0.0	0.1	26.3	8.3	114.06	156.78	114.43
1RS7_zinc42689701_Evo_9	376.07	26.01	253.89	0.1	0.1	9.8	14.5	125.62	136.83	133.33
1RS7_zinc42689701_Evo_10	381.72	16.51	1090	0.0	0.0	66.0	23.1	129.56	129.44	123.86

	1NSI	1RS7	3DQS						1NSI	1RS7	3DQS
AutoDocks	iNOS	nNOS	eNOS	n/e	n/i	e/n	i/n	iNOS	nNOS	eNOS	
1RS7_zinc71786250_Evo_1	13.13	21.69	4.69	4.6	1.7	0.2	0.6	160.19	159.18	157.18	
1RS7_zinc71786250_Evo_2	15.82	10.59	10.1	1.0	0.7	1.0	1.5	145.38	150.09	148.59	
1RS7_zinc71786250_Evo_3	23.19	3.98	3.36	1.2	0.2	0.8	5.8	151.68	146.56	140.86	
1RS7_zinc71786250_Evo_4	18.26	16.14	2.29	7.0	0.9	0.1	1.1	150.40	148.34	144.16	
1RS7_zinc71786250_Evo_5	15.73	22.27	4.97	4.5	1.4	0.2	0.7	145.47	153.41	156.57	
1RS7_zinc71786250_Evo_6	9.89	16.05	4.38	3.7	1.6	0.3	0.6	145.57	143.35	139.95	
1RS7_zinc71786250_Evo_7	19.57	8.78	2.56	3.4	0.4	0.3	2.2	155.80	159.09	150.85	

1RS7_zinc71786250_Evo_8	27.06	16.31	3.72	4.4	0.6	0.2	1.7	143.33	158.86	157.15
1RS7_zinc71786250_Evo_9	7.12	19.15	11.27	1.7	2.7	0.6	0.4	137.34	133.86	131.94
1RS7_zinc71786250_Evo_10	17.94	2.39	2.95	0.8	0.1	1.2	7.5	123.28	136.83	134.22

	1NSI	1RS7	3DQS					1NSI	1RS7	3DQS
AutoDocks	iNOS	nNOS	eNOS	n/e	n/i	e/n	i/n	iNOS	nNOS	eNOS

1RS7_zinc04859564_Evo_1	35.58	10.82	15.28	0.7	0.3	1.4	3.3	52.96	154.76	132.26
1RS7_zinc04859564_Evo_2	50.23	13.32	12.61	1.1	0.3	0.9	3.8	57.65	125.02	116.01
1RS7_zinc04859564_Evo_3	74.15	1.88	4.13	0.5	0.0	2.2	39.4	x	117.27	76.02
1RS7_zinc04859564_Evo_4	52.12	2.95	14.5	0.2	0.1	4.9	17.7	x	87.81	69.17
1RS7_zinc04859564_Evo_5	1370	36.71	311.62	0.1	0.0	8.5	37.3	x	147.39	119.60
1RS7_zinc04859564_Evo_6	1710	6.59	694.18	0.0	0.0	105.3	259.5	x	127.14	113.65
1RS7_zinc04859564_Evo_7	98.97	129.63	352.75	0.4	1.3	2.7	0.8	x	113.52	73.49
1RS7_zinc04859564_Evo_8	488.61	64.56	302.03	0.2	0.1	4.7	7.6	x	96.61	92.16
1RS7_zinc04859564_Evo_9	323.62	60.7	414.2	0.1	0.2	6.8	5.3	x	113.86	89.53
1RS7_zinc04859564_Evo_10	182.26	3.33	165.83	0.0	0.0	49.8	54.7	x	127.49	88.97

	1NSI	1RS7	3DQS					1NSI	1RS7	3DQS
AutoDocks	iNOS	nNOS	eNOS	n/e	n/i	e/n	i/n	iNOS	nNOS	eNOS

1RS7_zinc35335410_Evo_1	1030000	97060	56830	1.7	0.1	0.6	10.6	x	173.79	147.74
-------------------------	---------	-------	-------	-----	-----	-----	------	---	--------	--------

1RS7_zinc35335410_Evo_2	1040000	96370	57090	1.7	0.1	0.6	10.8	x	151.97	143.97
1RS7_zinc35335410_Evo_3	1040000	101770	56850	1.8	0.1	0.6	10.2	x	145.95	125.37
2RS7_zinc35335410_Evo_4	1040000	96650	56900	1.7	0.1	0.6	10.8	x	x	141.47
1RS7_zinc35335410_Evo_5	1040000	96340	56810	1.7	0.1	0.6	10.8	x	110.73	149.42
1RS7_zinc35335410_Evo_6	1040000	96560	56890	1.7	0.1	0.6	10.8	x	116.45	144.99
1RS7_zinc35335410_Evo_7	1040000	96240	56900	1.7	0.1	0.6	10.8	x	92.07	145.05
0RS7_zinc35335410_Evo_8	1050000	96810	56950	1.7	0.1	0.6	10.8	x	x	162.24
1RS7_zinc35335410_Evo_9	1040000	96390	56890	1.7	0.1	0.6	10.8	x	158.43	x
2RS7_zinc35335410_Evo_10	1040000	96360	56870	1.7	0.1	0.6	10.8	x	x	128.56

	1NSI	1RS7	3DQS					1NSI	1RS7	3DQS
AutoDocks	iNOS	nNOS	eNOS	n/e	n/i	e/n	i/n	iNOS	nNOS	eNOS
3DQS_zinc00081090_Evo_1	160.73	6.03	144.67	0.0	0.0	24.0	26.7	92.59	131.34	129.05
3DQS_zinc00081090_Evo_2	222.35	35.41	240.09	0.1	0.2	6.8	6.3	112.52	136.54	137.78
3DQS_zinc00081090_Evo_3	107.08	35.8	151.36	0.2	0.3	4.2	3.0	94.17	146.11	137.53
3DQS_zinc00081090_Evo_4	264.51	2.57	5.96	0.4	0.0	2.3	102.9	95.68	146.36	122.29
3DQS_zinc00081090_Evo_5	190.24	2.73	30.4	0.1	0.0	11.1	69.7	117.74	141.49	153.81
3DQS_zinc00081090_Evo_6	346.9	1.27	10.88	0.1	0.0	8.6	273.1	x	119.19	115.44
3DQS_zinc00081090_Evo_7	998.95	3.76	993.86	0.0	0.0	264.3	265.7	x	122.67	125.47

3DQS_zinc00081090_Evo_8	774.82	3.79	346.72	0.0	0.0	91.5	204.4	100.50	134.99	122.20
3DQS_zinc00081090_Evo_9	870.74	35.52	291.43	0.1	0.0	8.2	24.5	102.28	132.40	132.95
3DQS_zinc00081090_Evo_10	1540	15.5	186.37	0.1	0.0	12.0	99.4	135.83	140.75	139.65
	1NSI	1RS7	3DQS					1NSI	1RS7	3DQS
AutoDocks	iNOS	nNOS	eNOS	n/e	n/i	e/n	i/n	iNOS	nNOS	eNOS
3DQS_zinc12546533_Evo_1	8850	8180	8160	1.0	0.9	1.0	1.1	x	112.80	111.16
3DQS_zinc12546533_Evo_2	330.06	167.64	192.65	0.9	0.5	1.1	2.0	x	139.08	107.56
3DQS_zinc12546533_Evo_3	8840	8200	8160	1.0	0.9	1.0	1.1	x	140.93	133.15
3DQS_zinc12546533_Evo_4	8830	8190	8150	1.0	0.9	1.0	1.1	x	x	78.26
3DQS_zinc12546533_Evo_5	8860	8210	8150	1.0	0.9	1.0	1.1	x	126.44	129.35
3DQS_zinc12546533_Evo_6	8840	8190	8160	1.0	0.9	1.0	1.1	x	140.80	132.60
3DQS_zinc12546533_Evo_7	8840	8170	8140	1.0	0.9	1.0	1.1	x	110.26	122.31
3DQS_zinc12546533_Evo_8	332.15	168.18	330.07	0.5	0.5	2.0	2.0	x	82.44	115.73
3DQS_zinc12546533_Evo_9	330.65	126.1	321.43	0.4	0.4	2.5	2.6	x	101.13	106.46
4DQS_zinc12546533_Evo_10	542.62	224.22	334.12	0.7	0.4	1.5	2.4	x	x	121.61

Table 14: AutoDock results of evolved drug candidates in Fragment based De Novo Design.

1. Alignments

Sequence alignments show us how the three isoforms are different on the lower level. The table represents the residue similarity of the three isoforms sequences. The SASA script is intended to work on a receptor molecule in which binding site objects have been defined. The script converted the binding site points into potassium atoms. It calculated the Solvent Accessible Surface Area for all the amino acid residues in the receptor both in the presence of the binding site atoms and in their absence. The difference is the surface area of atoms lining the cavity. This area is reported in the standard output of the script as well as in the Binding Site tab of the data table as the 'Cavity SASA' of the selected/visible binding site object. We found opportunity to compare the binding site shape and volume of the NOS isozymes. The positioning of the atoms are presented in the figure 3.12.

For cavity study, we used 1FOI eNOS, 3B3M as nNOS and 1NSI for the iNOS

NOS Alignments	eNOS/nNOS	eNOS/iNOS	nNOS/iNOS	nNOS/iNOS/eNOS
# of Identical aa	276	248	275	221
% identity	65.56	58.91	65.48	52.49

Table 15: NOS isozymes active site similarities

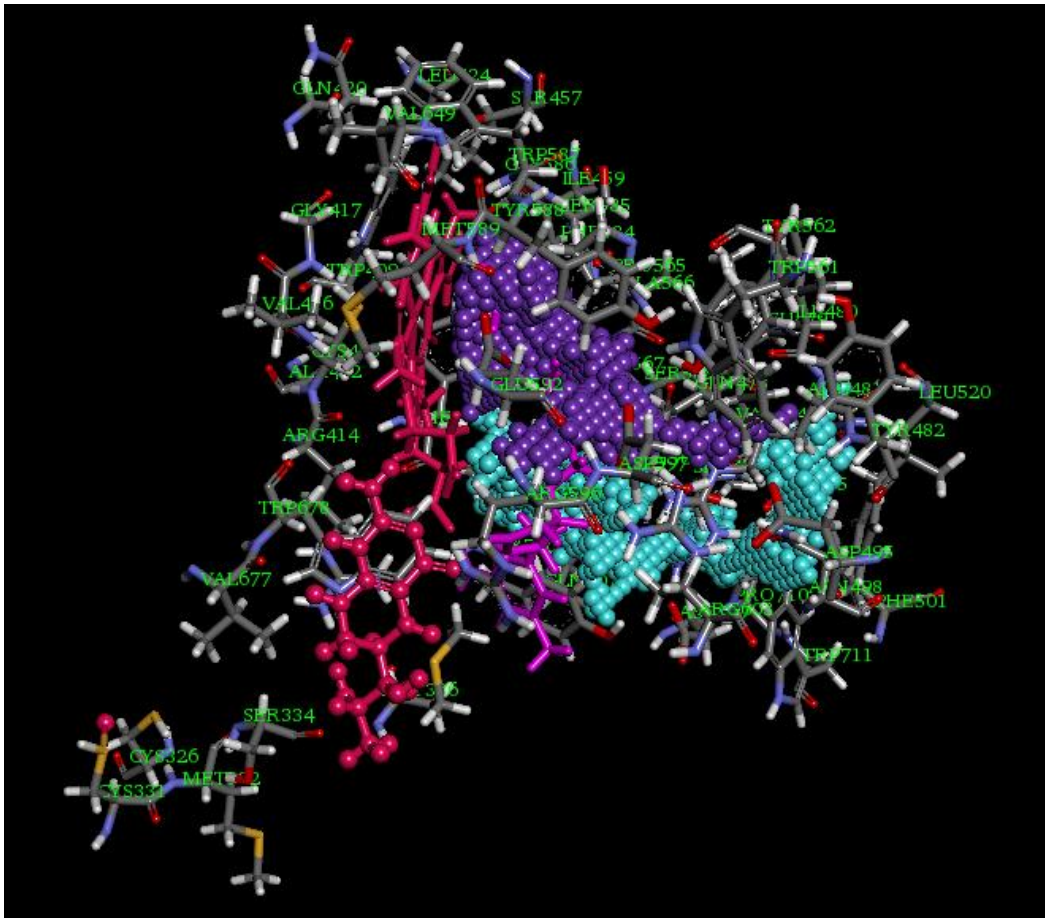


Figure 24: nNOS active site cavity and positioning of the close residues

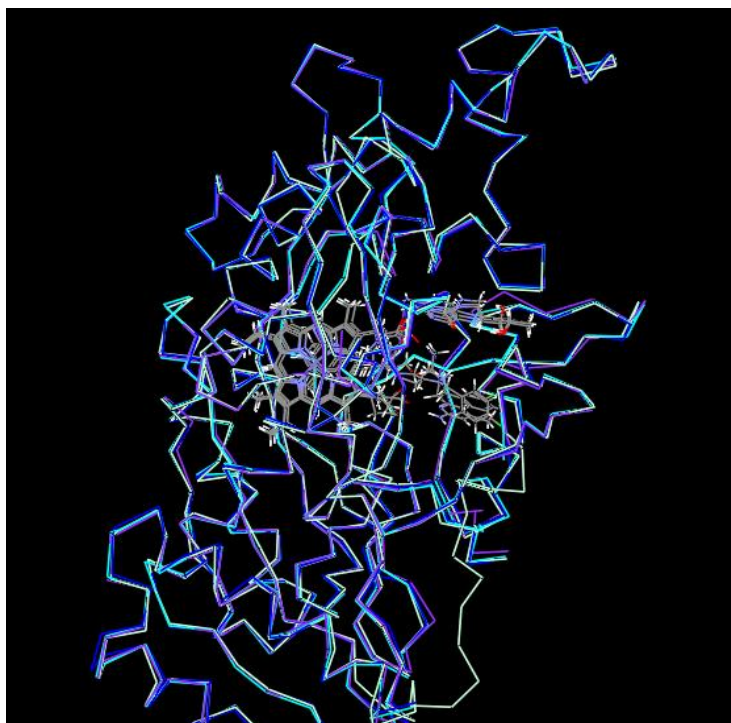


Figure 25: Five structurally aligned eNOS enzymes

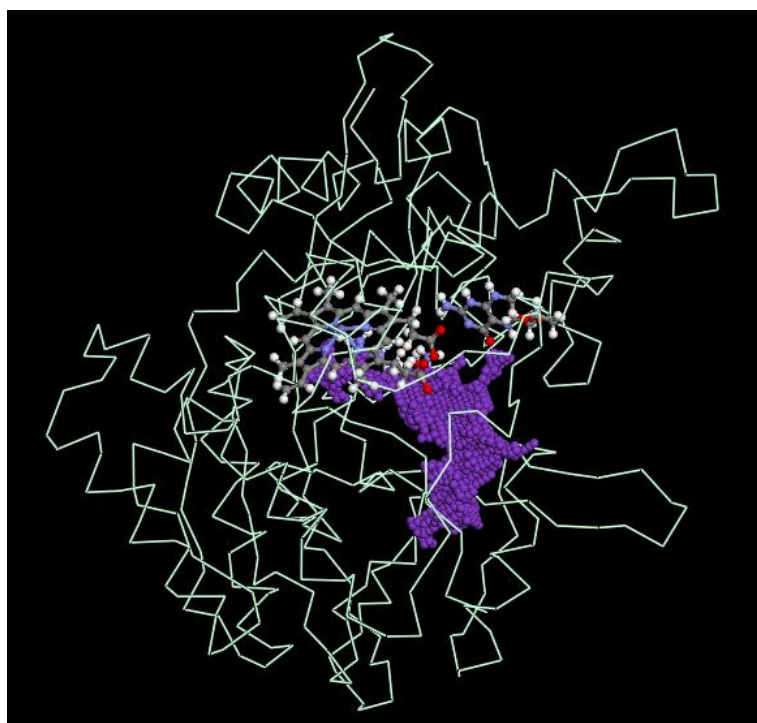


Figure 26: eNOS enzymes with its cofactors and cavity

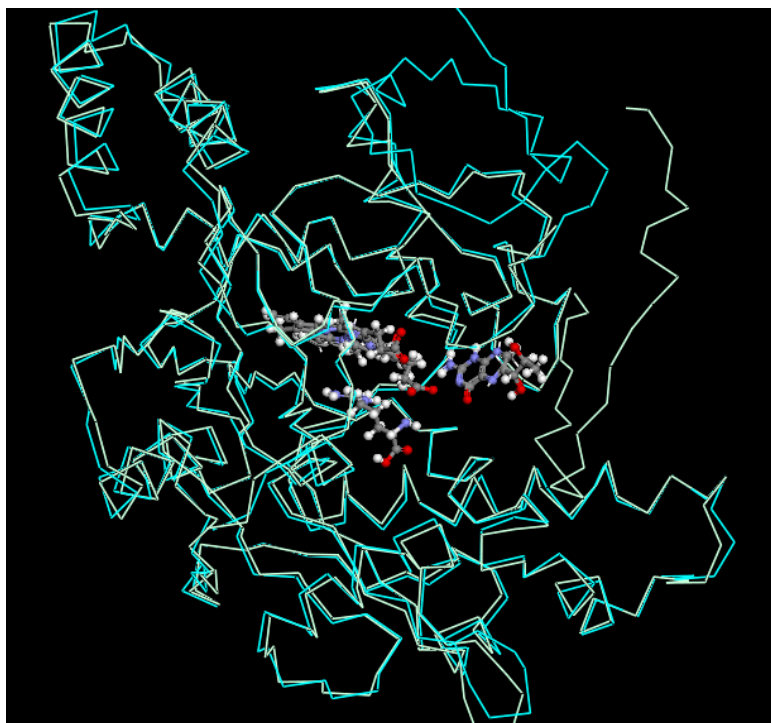


Figure 27: Two structurally aligned iNOS enzymes

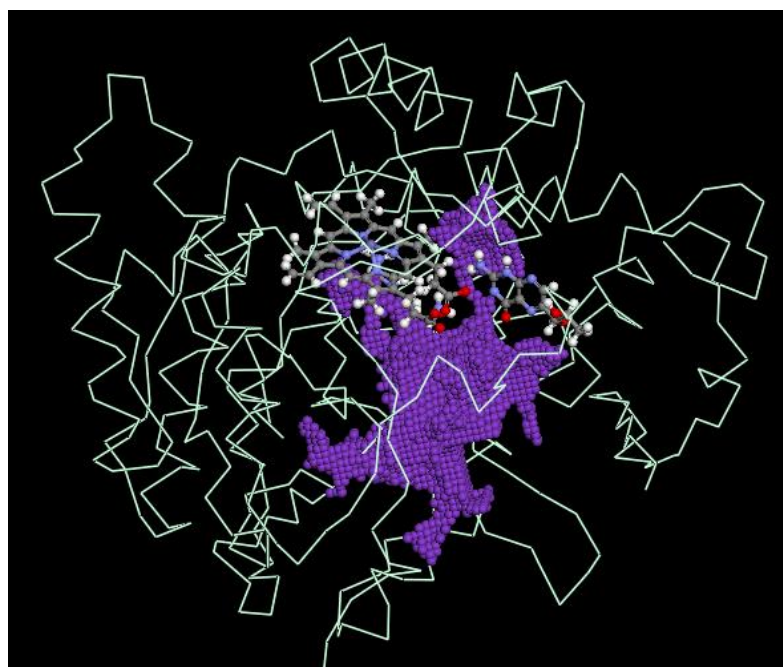


Figure 28: iNOS enzymes with its cofactors and cavity

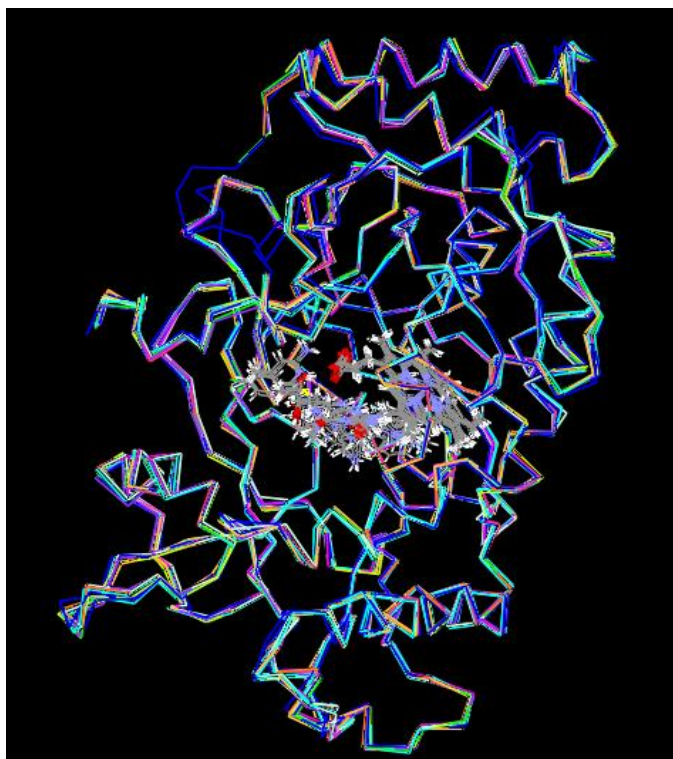


Figure 29: Ten structurally aligned nNOS enzymes

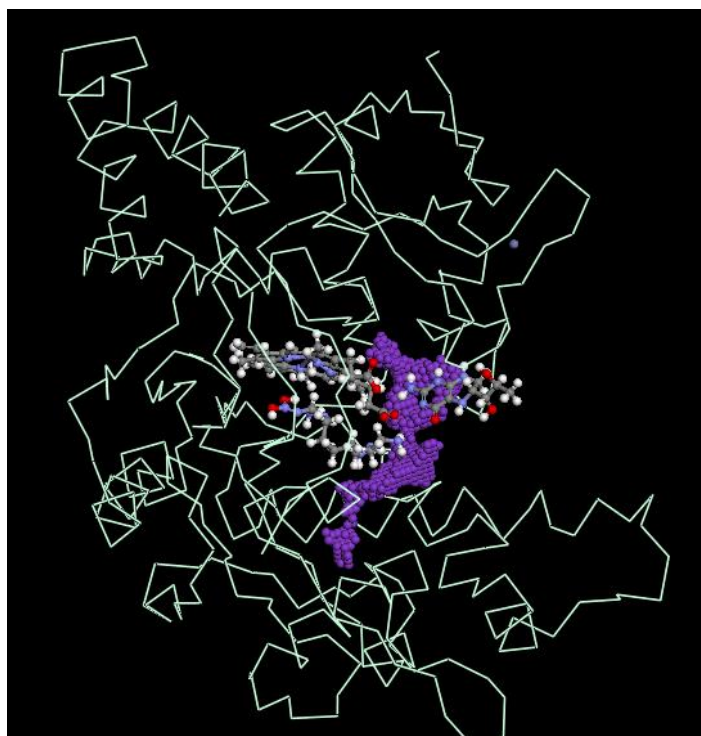


Figure 30: nNOS enzymes with its cofactors and cavity

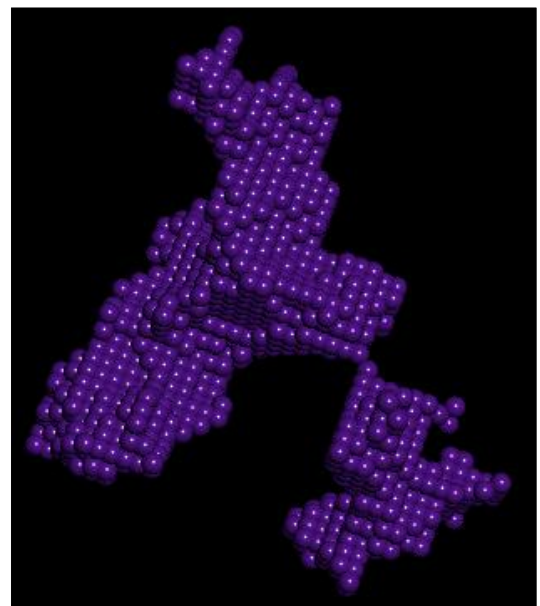
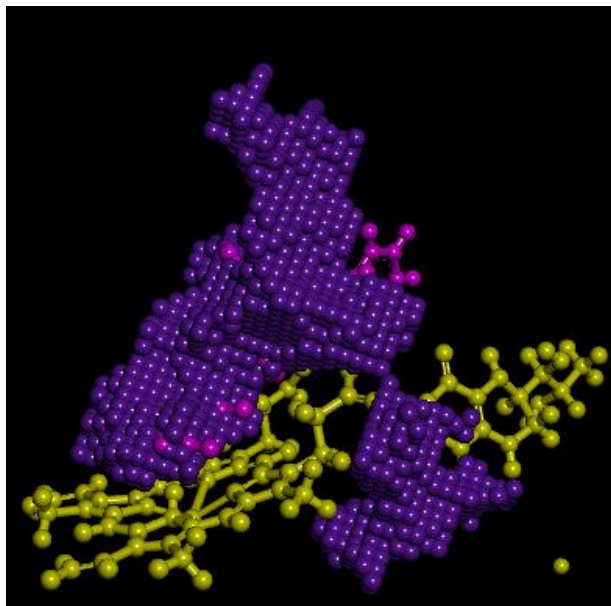
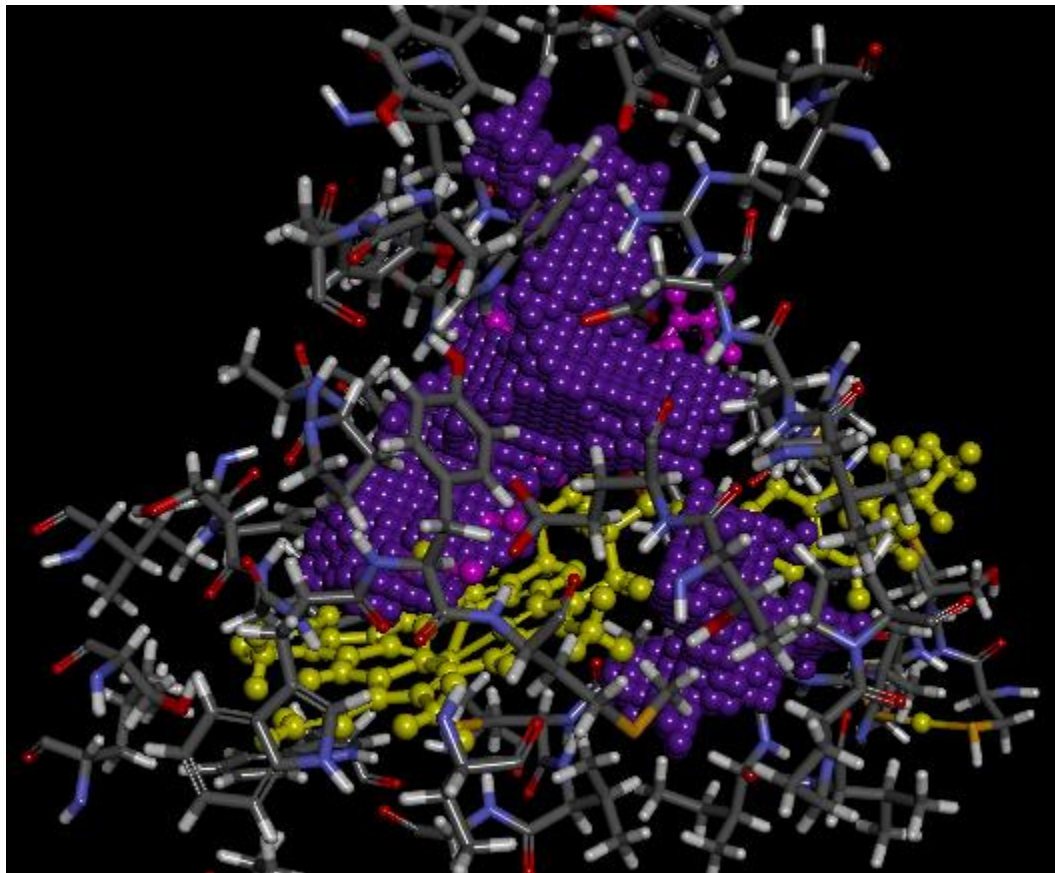


Figure 31: nNOS Cavity

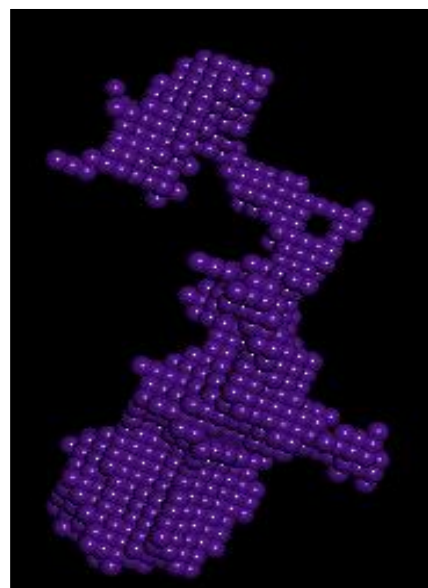
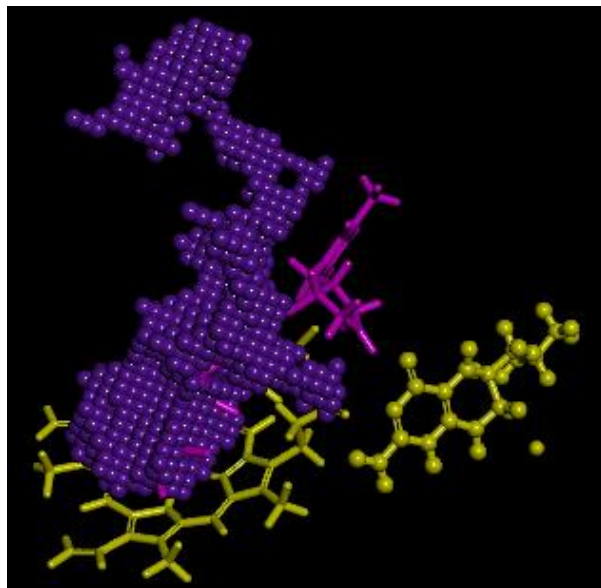
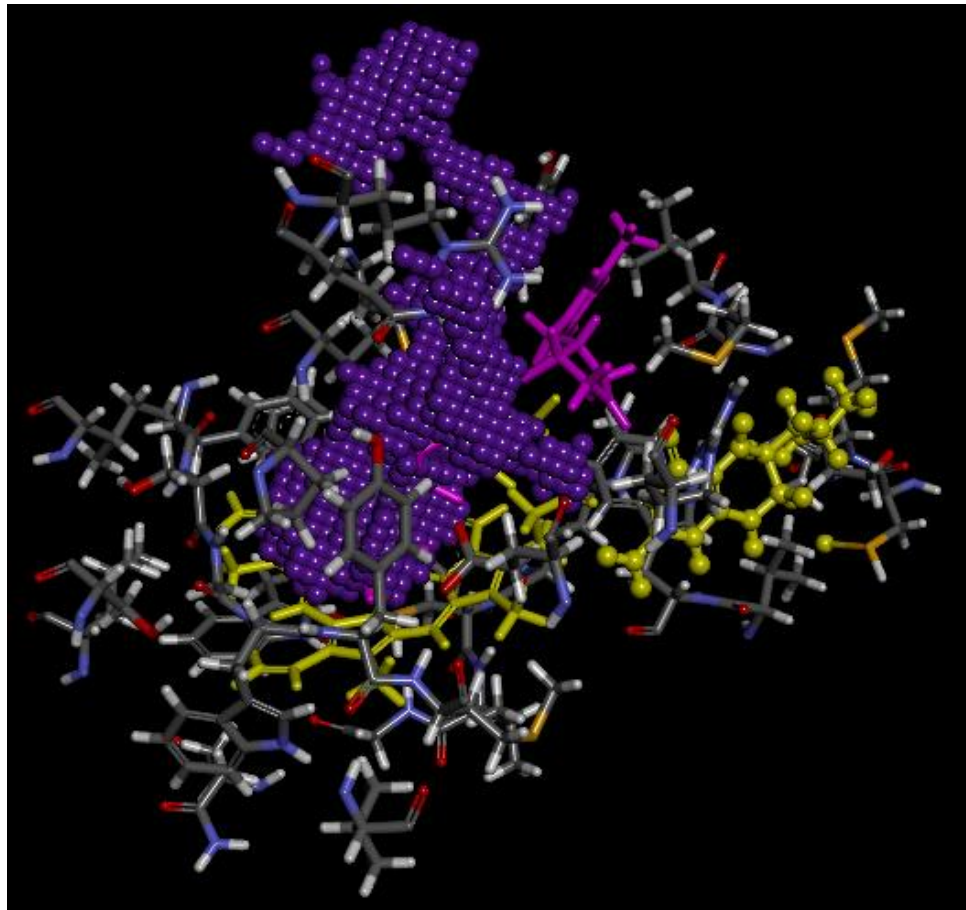


Figure 32: eNOS Cavity

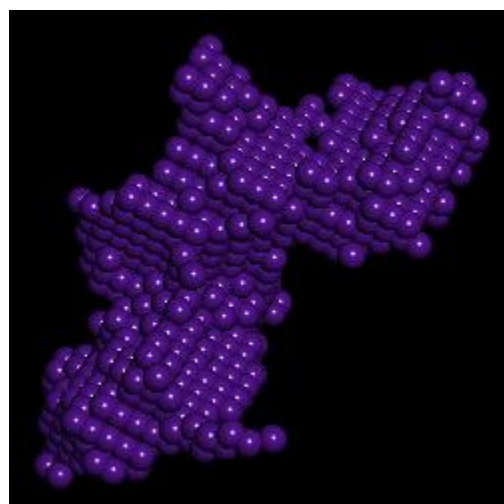
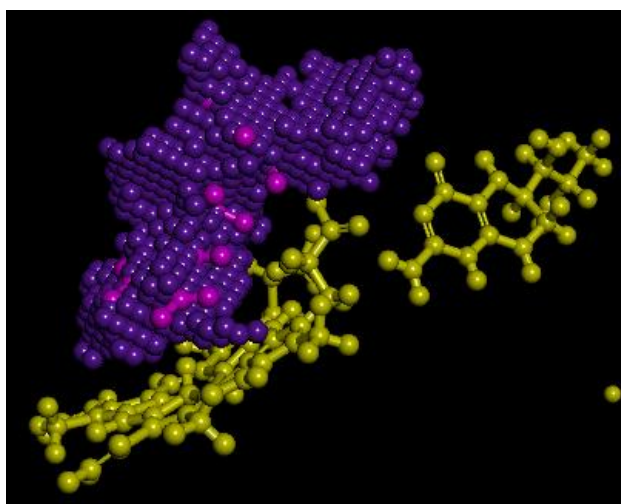
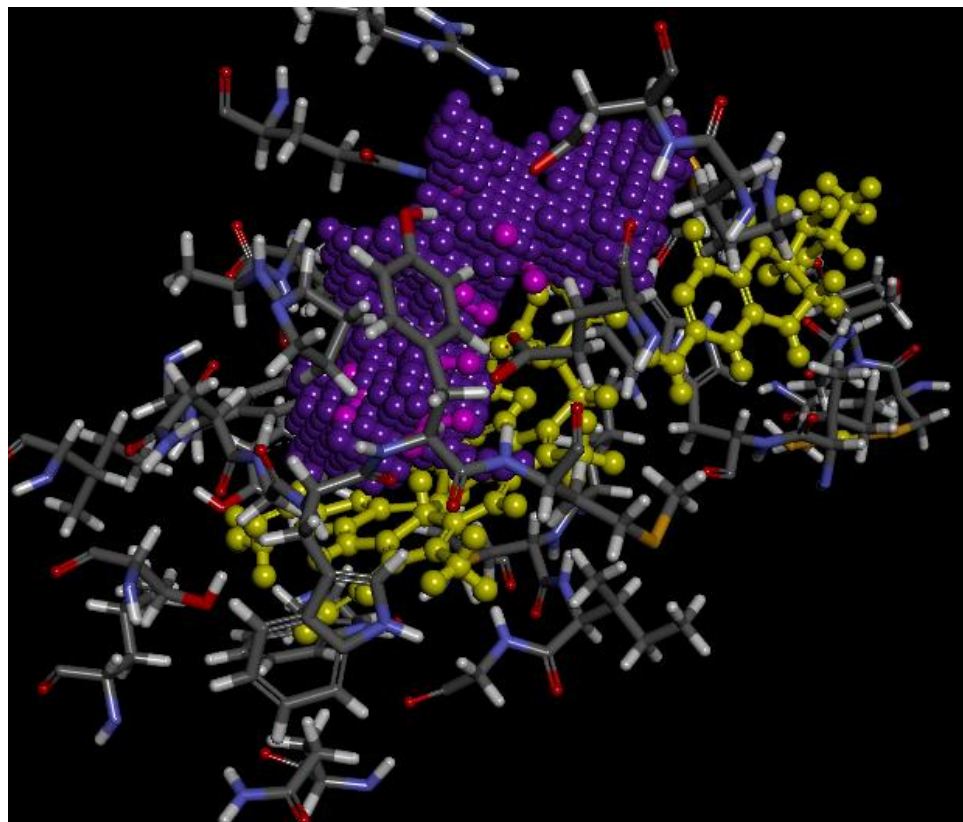


Figure 33: iNOS Cavity

4 Conclusion

n/e (nNOS to eNOS) and i/n (iNOS to nNOS) K_i ratios are representing selectivity which is the ratio of binding energies of the bindings of one ligand to two different isozymes. Smaller AutoDock binding results matches with larger CDOCKER/LibDock scores, which are not linear in the comparison but exponential. Furthermore, among all these docking computations, very seldom we get conflicting docking calculation results that gave negative scores for CDOCKER. This shows that our ligands structures, ligand minimization techniques, optimization environments, and enzyme choices are good enough to create a ligand model. Spartan quantum calculations, Accelrys ligand preparation and AutoDock Gasteiger charges seem to be suitable.

In our computational environment, rigid proteins and rigid ligand are used because flexible docking needs more computational power. As in the key lock analogy, we placed ligand groups into binding site cavities. In binding process, entropy of the environment facilitates binding action, but in silico environment we can't consider entropic effect of outside water molecules because of the implementation difficulties. We fixed only a few H₂O molecules next to specific amino acids in the binding region during the AutoDock dockings. This directed us to slightly better AutoDock results. Contrary in Accelrys, it did not help because the methods of Accelrys protocols works in a different way as mentioned and the fixed water molecules blocks the docking operation in Accelrys' dynamic programming algorithm.

One of the challenging outcome of this study showed that NOS is a difficult simulation problem. Enzymes usually have one or two cofactors. Having 5 cofactors and water molecular interactions, there are many indefinite parameters in the problem. In 3D images, we can see folding of some big ligands in one of the two cavities of NOS enzyme. For emerging of this kind of conformations enzyme should have a specific mechanisms that with only one amino acid movement the receptor turns out to be a door opening to binding.

At the end of de novo designs, we discovered ten new nNOS selective inhibitors candidates. The selectivity ratios are changing from 15 to 20 times to a few hundred times, which are comparably promising inhibition capacities to the past experimental binding data.

A few of the high selective compounds like “1RS7_zinc39941619_Evo_10” and “1NSI_zinc04649158_evo4” had great selectivity ratios over 400 times against both iNOS and eNOS at the end of docking results. On the other hand, the ADMET results were very poor for them that it is not possible them to reach the target enzyme in the body. ADMET measured if the compounds will be able to move to the target passing Brain Blood Barrier and intestinal absorption. We eliminated 6 of the 16 finalist compounds. All remaining 10 compounds did very well with both inhibitions and selectivity tests.

There were four evolutionary path for the remaining 10 compounds. Three of them evolved from “zinc42689701” molecule in 1RS7 nNOS, three of them evolved from

“zinc00151524” molecule in 1NSI iNOS, the remaining three of them evolved from zinc04859564 in 1RS7 and the final last one of them evolved from zinc00081090 in 3DQS eNOS enzyme. This last one named “3DQS_zinc00081090_Evo8” yielded the best evolutionary results as 91 and 204 times selectivity against eNOS and iNOS having 3.79 nm inhibition k_i value in AutoDock and 134 to 122 and to 100 CDock scores.

1RS7_zinc42689701_Evo_3 from the group of first three, 1NSI_zinc00151524_evo7 from the group of second three and 1RS7_zinc04859564_Evo_6 from last group of last three outputted as (e/n:59.5, i/n:72.8 k_i :34nm), (e/n: 114, i/n:55, k_i :6.28nm), (e/n: 105, i/n:259, k_i :6.59nm) respectively. CDock scores show that they had higher score values as 133 to 116 and 124, 113 to 73 and 127 to 113 respectively.

2D and 3D images of these novel compounds gave us some clues about how they manage to bind to cavity. 1NSI_Zinc00151524_Evo3 compound is binding to active site by a pi-sigma bond to Heme and an ASN354 hydrogen bond in one side, and with many pi-cation interactions to aromatic rings by ARG388 in the other side.

Zinc00151524_Evo7 compound is binding to active site by the same pi-sigma bond to Heme, a TYR491 pi-pi bond to the first ring and an ASN352 hydrogen bond instead of ASN354 in one side, and with many pi-cation interactions to aromatic rings by ARG388, ARG266 and TYR373, TRP346 hydrogen bonds in the other side. Evo10 of this group is binding to active site by ASN354 and additional ALA262 hydrogen bonds as similar to Evo3 in one side and with the same pi-cation and HBounds same as Evo7 in the other side. Figure 14, Figure 15 and Figure 16 also denotes the electrostatic, polar

interactions in pink, van der waals effect in green and SASA surfaces in blue. Binding of second and third group which evolved from zinc04859564 and zinc42689701 in 1RS7 are have similar pii-pi, pi-cation, pi-sigma and hydrogen bounds as shown in figures Figure 17,18,19,20,21 and 22. ARG414, ARG596, ARG603, ARG481, TRP678, TYR588, TYR706 and ASN569 are the key amino acids in these groups. Different from the other groups we observed H4B hbond interaction for these cases. Our best selective ligand 3DQS_ zinc00081090_Evo8 had strong pi interactions in the central ring to ARG185, ARG252 and Heme and hbonds to GLU363 in the central region. His one of the forked front ring stabilizes itself TYR359 pi interaction. All these amino acids mentioned here are seems to have primary importance in NOS binding processes.

Our active site cavity comparisons stated in Table 15 show us nNOS cavity has most similar to the other isozymes. But it seems that differences to eNOS is not matching to the iNOS since iNOS and eNOS are not as similar as they are similar to nNOS. nNOS is %65 similar to eNOS and iNOS in the active site where as iNOS is %58 similar to eNOS in the active site.

Most common amino acids in active sites also detected at the end of alignment procedures. They are as follows:

Among 5 eNOS enzymes based on 1FOI: VAL106, LEU107, Pro108, ARG109, Leu111, GLN112, ARG114, ARG185, CYS186, VAL187, ARG244, Ile245, Trp246, Asn247, SER248, GLN249, VAL251, ARG252, TYR253, ASP266, ASN269, TRP332, TYR333, PRO336, ALA337, VAL338, VAL338, SER339, ASN340, MET341, PHE355, SER356, GLY357, TRP358, TYR359, MET360, THR362, GLU363, ARG367, ASN368, ASP371,

ARG374, TYR375, ALA448, TRP449, , LE450, VAL451, PRO452, PRO453, ARG476, TYR477, GLN478,
PRO479, ASP480, PRO481, TRP482

Among 2 iNOS enzymes based on 1NSI: TRP90, MET120, THR121, PRO122, LEU125, THR126,
ARG199, ILE201, ARG258, VAL259, TRP260, ASN261, ALA262, GLN263, LEU264, ILE265, ARG266, ASP280,
PRO281, ALA282, ASN283, VAL284, GLU285, PHE286, LEU289, VAL305, PRO306, LEU307, ILE321, TRP346,
TYR347, PRO350, ALA351, VAL352, ALA353, ASN354, MET355, PRO365, GLY366, CYS367, PRO368,
PHE369, ASN370, GLY371, TRP372, TYR373, MET374, THR376, GLU377, VAL380, ARG381, ASP382,
ASP385, GLN387, ARG388, HIS436, ILE462, TRP463, LEU464, VAL465, PRO466, PRO467, TYR491, GLN492,
VAL493, GLU494, ALA495, TRP496, LYS497

Among 10 nNOS enzymes based on 3B3M: THR321, LEU322, GLU323, THR324, CYS326,
MET332, GLY333, ILE335, MET336, LEU337, PRO338, THR342, ALA408, ASN411, ALA412, SER413,
ARG414, CYS415, VAL416, SER477, GLN478, ARG481, TYR482, ASP495, ALA497, ASN498, TRP561,
TYR562, PRO565, ALA566, VAL567, SER568, ASN569, MET570, LU573, PHE584, SER585, GLY586, TRP587,
TYR588, MET589, THR591, GLU592, Ile593, VAL595, ARG596, ASP597, ASP600, ARG603, TYR604, HIS651,
ALA654, THR655, Pro673, Asp675, VAL677, TRP678, ILE679, VAL680, PRO681, PRO682, VAL690, ASN697,
TYR698, ARG699, LEU700, THR701, PRO702, SER703, PHE704, GLU705, TYR706

We moved on with volumetric visualization of active sites of the enzymes. A Perl script run on Accelrys put potassium (K) atoms to the cavity volume in the active site to visualize the active site. The volumes are represented in Figure 31 to Figure 33. These cavities are exact active site pockets. In nNOS, eNOS and iNOS we used 2743, 1815 and 1429 units of potassium volumes. This will give us an idea of how the shape of main binding cavity. In addition shape of tunnels in NOS enzymes to reach active site pockets may be clear by comparing the Figure 26, Figure 28 and Figure 30 which visualize

aligned larger space to cavity volumes. The pinkish colors in the purple represent the ligand in the pocket. Figure 30

We now know the main pi-pi, Pi-Cation, hbond interactions of the systems and the active atoms holding the ligands in their specific binding location. We also know the similarity of the three different isozymes. We have ideas about the shape of the active sites. So in the further study one can use our ligands and investigate them in these cavities. Instead of de novo design, one can use a step by step approach with the geometric data we have in the hand. We can design new drug candidates by narrowing the de novo constraints according to these important interactions.

As a conclusion, introducing computational methods are precious to save the experimental time and establish a clear understanding about the molecules we are working on even though we cannot grab the complete picture. As an outcome of this study, we hope that our drug candidate inhibitors have the value to be tested in the further steps of experimental and clinical studies.

References

- GRID. (2002). *Version 20*. London, 4Chandos street, , U.K.: Molecular Discovery, Ltd.
- Abu-Soud, H. M., Presta, A., Mayer, B., & Stuehr, D. J. (1997, July). Analysis of Neuronal NO Synthase under Single-Turnover Conditions: Conversion of N¹⁵-Hydroxyarginine to Nitric Oxide and Citrulline. *Biochemistry*, *36*, 10811-10816.
- After, P. L., & Feldman. (1993). The surprising life of nitric oxide. *C&EN News*, *71*, 26-38.
- Arnet, U. A., McMillan, A., Dinerman, J. L., Ballermann, B., & Lowenstein, C. J. (1996, June). Regulation of Endothelial Nitric-oxide Synthase during Hypoxia. *The Journal Of Biological Chemistry*, *271*(25), 15069-15073.
- Batra, J., Chatterjee, R., & Ghosh, B. (2007, Oct). Inducible nitric oxide synthase (iNOS): role in asthma pathogenesis. *Indian J Biochem Biophys.*(44(5)), 303-9.
- Böhm, H. (1992). The computer program LUDI: A new method for the de novo design of enzyme inhibitors. *Comput - Aided Mol. Design*(6), 61-78.
- Brooks, B. R., Bruccoleri, R. E., Olafson, B. D., States, D. J., Swaminathan, S., & Karplus, M. (1983). CDocker. *J. Comput. Chem.*(4), 187-217.
- Chirkov, Y. (2001, Jun 1). Stable angina and acute coronary syndromes are associated with nitric oxide resistance in platelets. *J Am Coll Cardiol*(37(7)), 1851-7.
- Drummond, G., Cai, H., Davis, M., & Ramasamy, S. (2000, Feb 18). Transcriptional and posttranscriptional regulation of endothelial nitric oxide synthase expression by hydrogen peroxide. *Circulation Research*, *3*(86), 347-54.
- Erdal, E. P., Litzhger, E. A., Seo, J., Zuhu, Y., Ji, H., & Silverman, R. B. (2005). Selective neuronal nitric oxide synthase inhibitors. *Curr Top Med Chem.*(5), 603-624.
- Fengtian, X., James, K. M., Kristin, L. J., Ji, H., Mataka, J., Xia, G., et al. (2011, 4). Improved Synthesis of Chiral Pyrrolidine Inhibitors and Their Binding. *American Chemical Society*, *54*, 6399.
- Fleming, I., & Busse, R. (2003, Jan). Molecular mechanisms involved in the regulation of the endothelial nitric oxide synthase. *American Journal of Physiology*, 284.
- Gachhui, R., Ghosh, D. K., Wu, C., Parkinson, J., Crane, B. R., & Stuehr, D. J. (1997, April). Mutagenesis of Acidic Residues in the Oxygenase Domain of Inducible Nitric-Oxide Synthase Identifies a Glutamate Involved in Arginine Binding. *Biochemistry*, *36*(17), 5098.
- Hah, J.-M., Martasek, P., Roman, L. J., & Silverman, R. B. (2003, 7). Aromatic Reduced Amide Bond Peptidomimetics as Selective Inhibitors of Neuronal Nitric Oxide Synthase. *J. Med. Chem.*, *46*, 1661-1669.
- Huang, P. L., Huang, Z., Mashimo, H., Bloch, K. D., Moskowitz, M. A., Bevan, J. A., et al. (1995). Hypertension in mice lacking the gene for endothelial nitric oxide

- synthase. *Nature*, 377, 239-242.
- Ji, H., Li, H., Flinspach, M., Poulos, T. L., & Silverman, R. B. (2003, 6). Computer Modeling of Selective Regions in the Active Site of Nitric Oxide Synthases: Implication for the Design of Isoform-Selective Inhibitors. *J. Med. Chem.*, 46, 5700-5711.
- KA, P. (2012, Jan). The effects of modulating eNOS activity and coupling in ischemia/reperfusion (I/R). *Naunyn-Schmiedeberg's archives of pharmacology*, (1)(385), 27-38.
- Kowaluk, E. A., Daanen, J. F., Kohlhaas, K. L., Alexander, K. M., Wagenaar, F. L., Kerwin, J. F., et al. (1998, 1). Nitroaromatic Amino Acids as Inhibitors of Neuronal Nitric Oxide Synthase. *J. Med. Chem*, 41(14), 2636--2642.
- Lee, S., Oplinger, J. A., Frick, L. W., Garve, E. P., Furfine, E. S., & Shearer, B. G. (1997, November). Substituted N-Phenylisothioureas: Potent Inhibitors of Human Nitric Oxide Synthase with Neuronal Isoform Selectivity. *J. Med. Chem*, 40, 1901-1905.
- Li, H., Raman, C. S., Martasek, P., Masters, B. S., & Poulos, T. L. (2001, January 19). Crystallographic studies on endothelial Nitric Oxide complexed with nitric oxide and mechanism-based inhibitors. *Biochemistry*, 40(18), 5399-5406.
- Li, H., Shirnizu, H., Flinspach, M., Jamal, J., Yang, W., Xian, M., et al. (2002). The novel binding mode of N-Alkyl-N-Hydroxyguanidine to neuronal nitric oxide synthase provides mechanistic insights into NO biosyntheses. *Biochemistry*, 41, 13868-13875.
- Olken, N. M., Osawa, Y., & Marletta, M. A. (1994). Characterization of the Inactivation of Nitric Oxide Synthase by NG-Methyl-L-arginine: Evidence for Heme Loss. *Biochemistry*, 33(49), 14784-14791.
- RA, C., Congreve, M., Murray, C., & Rees, D. (2005, July 15). Fragment-based lead discovery: leads by design. *Drug Discov Today*(10), 987-992.
- RA, C., Congreve, M., Murray, C., & Rees, D. (2005 Jul 15). Fragment-based lead discovery: leads by design. *Drug Discov Today*, 987-992.
- Schulz, R., Nava, E., & Moncada, S. (1992). Induction and potential biological relevance of a Ca²⁺ -independent nitric oxide synthase in the myocardium. *Br. J. Pharmacol.*, 105, 575-580.
- Shearer, B. G., Oplinger, J. A., Lee, S., Garvey, E. P., Salter, M., Duffy, C., et al. (1998, 1). N-Phenylamidines as Selective Inhibitors of Human Neuronal Nitric Oxide Synthase: Structure-Activity Studies and Demonstration of in Vivo Activity. *J. Med. Chem.*, 41(15), 2858-2871.
- Silverman, R. B. (2009, March). Design of selective neuronal nitric oxide synthase inhibitors for the prevention and treatment of neurodegenerative diseases. *Accounts of Chemical Research*, 42(3), 439-451.
- Silverman, R. B., & Zhu, Y. (2008, Feb 26). Revisiting Heme Mechanisms. A Perspective on the Mechanisms of Nitric Oxide. *Biochemistry*, 47, 2232.

- Silverman, R. B., Igarashi, J., Li, H., Jamal, J., Ji, H., Fang, J., et al. (2009). Crystal Structures of Constitutive Nitric Oxide Synthases in Complex with De Novo Designed inhibitors. *J. Med. Chem.*, *52*, 2060-2066.
- Silverman, R. B., Martasek, Roman, Huang, & Hui. (2000, 3). Synthesis and Evaluation of Peptidomimetics as Selective Inhibitors and Active Site Probes of Nitric Oxide Synthases. *J. Med. Chem.*, *43*, 2938-2945.
- Silverman, R. B., Poulos, T. L., Jamal, J., Li, H., Xue, F., & Delker, S. L. (2010). Role of Zinc in Isoform-Selective Inhibitor Binding to. *Biochemistry*, *49*(51), 10803--10810.
- Silverman, R. B., Poulos, T. L., Roman, L. J., Martásek, J., Xue, F., Huang, J., et al. (2010, 3). Structure-based design, synthesis, and biological evaluation of lipophilic-tailed. *Bioorganic & Medicinal Chemistry*, *18*, 6526--6537.
- Silverman, R. B., Roman, L. J., Martasek, P., Gomez-Vidal, J. A., & Ji, H. (2006, 4). Conformationally Restricted Dipeptide Amides as Potent and Selective Neuronal Nitric Oxide Synthase Inhibitors. *J. Med. Chem.*, *49*(21), 6254-6263.
- Silverman, R. R., Seo, J., Igarashi, J., Li, H., Martasek, P., Poulos, T. L., et al. (2007, 11). Structure-Based Design and Synthesis of Nö-Nitro-L-Arginine-Containing Peptidomimetics as. *J. Med. Chem*, *50*(9), 2089-2099.
- Silverman, R. B., Ji, H., Stanton, B. Z., Igarashi, J., Li, H., Martasek, P., et al. (2008). Minimal Pharmacophoric Elements and Fragment hopping, an approach directed at Molecular Diversity and Isozyme Selectivity. Design of Selective Neuronal Nitric Oxide Synthase Inhiitors. *J.Am.Chem. Soc.*, *130*, 3900-3914.
- Sousa, S., & Fernandes, P. (2006, 10). Protein-ligand docking: current status and. *Wiley Online Library*, *1*(65), 15–26.
- Teng, X., Zhang, H., Snead, C., & Catravas, J. (2002, Jan). Molecular mechanisms of iNOS induction by IL-1 beta and IFN-gamma in rat aortic smooth muscle cells. *Am J Physiol Cell Physiol*.(282), 144-52.
- Tierney, D. L., Huang, H., Martasek, P., Roman, L. J., Silverman, R. B., & Hoffman, B. M. (2000). ENDOR spectroscopic evidence for the geometry of binding of retro-inverso-Nw-nitroarginine-containing dipeptid amides to neuronal nitric oxide synthase. *J.Am.Chem.Soc.*, *122*, 7869-7875.
- Westerhuis, J. A., Kourti, T., & Macgregor, J. F. (1998). Analysis of multiblock and hierarchical PCA and PLS models. *J. Chemom.*(12), 301-321.
- Wolff, D. J., Gauld, D. S., Neulander, M. J., & Southan, G. (1997, June). Inactivation of Nitric Oxide Synthase by Substituted Aminoguanidines and Aminoisothiouras. *The Journal Of Pharmacology and Experimental Therapeutics*, *283*(1), 265-273.
- Zhang, H. Q., Fast, W., Marletta, M. A., Martasek, P., & Silverman, R. B. (1997, 8). Potent and Selective Inhibition of Neuronal Nitric Oxide Synthase by Nö-Propyl-L-arginine. *J. Med. Chem.*, *40*, 3869-3870.

Curriculum Vitae

Ali Bora Büyüktürk is a graduate of Pertevniyal High School. He received his first BS&MS degrees from Boğaziçi University in Teaching Physics Department in 2004. Next, he got his second BS degree from Istanbul Bilgi University in Computer Science Department in 2010 and second M.S. degree in 2013 in Computational Biology and Bioinformatics Graduate Program from Kadir University. Before 2010 he was working as a part time physics teacher in different high schools. He worked as a research assistant at the IT department of Kadir Has University from 2010 to 2012. During this time, he has been assisting IT programming courses and taking place in bioinformatics research projects. His research interests include algorithms, programming languages, computer graphics and drug design.